IOP Publishing Measurement Science and Technology
Meas. Sci. Technol. **31** (2020) 042001 (20pp) https://doi.org/10.1088/1361-6501/ab4c10

Topical Review

Prospects of photonic crystal fiber for analyte sensing applications: an overview

Moutusi De[1], Tarun Kumar Gangopadhyay[2] and Vinod Kumar Singh[1]

[1] Optical Fiber Laboratory, Department of Physics, Indian Institute of Technology (Indian School of Mines), Dhanbad 826004, India
[2] Former Senior Principal Scientist of Fiber Optics and Photonics Division, CSIR-Central Glass and Ceramic Research Institute, CSIR, Kolkata 700032, India

E-mail: demoutusi@gmail.com (MD), tkg@cgcri.res.in (TKG) and vksingh@iitism.ac.in (VKS)

Received 9 January 2019, revised 22 September 2019
Accepted for publication 8 October 2019
Published 8 January 2020

Abstract

The detection and monitoring of physical, chemical and biomedical parameters are increasingly reliant on fiber-optic sensing technology. Of applicable optical methods, photonic crystal fiber (PCF) sensors show its potential as a sensitive technique in environmental, industrial, food preservation and medical applications. Such a system incorporates the fabrication of a particular PCF, the interaction of wave propagation with the measured field, signal processing to offer automated real-time measurement in terms of the amplitude, phase, polarization and wavelength of spectrum.

This article is an endeavour towards giving a brief overview of the development of analyte sensors using PCFs in the last few years. Different kinds of PCF analyte sensors are discussed based on the measuring entity and reported works. This discussion integrates a variety in the nature of the core, metal coating on the PCF and liquid infiltration in the holes. It is also considered to present the phenomena of its internal structure and interference techniques for several applications. Advances in this technology, particularly in the areas of gas sensing, chemical spices and bio analytes, will be discussed in this article with some applications.

Keywords: photonic crystal fiber, interferometry, surface plasmon resonance, fiber-optics sensor

(Some figures may appear in colour only in the online journal)

Abbreviations

PCF	Photonic crystal fiber
SC-PCF	Solid core photonic crystal fiber
HC-PCF	Hollow core photonic crystal fiber
NA	Numerical aperture
FBG	Fiber Bragg grating
TIR	Total internal reflection
FP cavity	Fabry–Pérot cavity
SMF	Single mode fiber
MMF	Multi-mode fiber
LMA	Large mode area
RI	Refractive index
MZI	Mach–Zehnder interferometer
SPR	Surface plasmon resonance
LC	Liquid crystal
PBG	Photonic band gap fiber
Hi-Bi	Highly birefringent
LPG	Long period grating
DC-PCF	Dual core photonic crystal fiber
MOF	Microstructure optical fiber
D-PCF	D-shaped photonic crystal fiber
LC-PCF	Liquid crystal photonic crystal fiber
SERS	Surface enhanced Raman scattering

1. Introduction

Fiber optics technology is one of the great branches of optics, especially in the twentieth century. Starting from the first low-loss single-mode waveguides in 1970, this technology expands itself at a tremendous rate in the field of communication, sensing, medicine delivery etc. Optical fiber-based sensors became very popular due to their high sensitivity, small size, flexibility, immunity to radio frequency and electromagnetic interference and they can be used in many unfavorable situations. But after some time, fiber optics technology faced some short degrees of freedom, such as, lack of variation of geometry and silica-based refractive index profile selection etc., which brings saturation in improving its optical characteristics [1].

Fiber-optic sensors are useful in many applications where electrical sensors cannot be used, such as microwave fields, high voltage devices, power plant, high radiation in atomic research area and mining industry applications, etc. These sensors can be used in environmental monitoring, controlling the soil heating process in the case of removing toxic organic compounds from an industrial area using radio waves, in magnetic resonance scanners (MRIs), in laser therapy, to ensure industrial safety in generators and transformers, especially in a harsh environment, to monitor chemical and petrochemical materials, during wood drying and in welding mechanism up to the gas detection in volcanoes to name a few.

Then after waiting for nearly three decades of development in photonic crystal fibers (PCFs), in 1996 Russell and his colleagues [2] provided a strong impulse in fiber optics technology towards a new beginning for versatile and improved applications. PCF is a relatively new wing of optical fiber technology and has drawn enough attention due to its flexible geometrical structure that led to many unique properties. These advance properties are useful in several fields of application. PCF sensor technology is one of them. Generally, PCF is made of only one material, silica. Its cladding region consists of many air holes along the cross section that run throughout the length of the fiber assuring the confinement of light in the core region. The construction of the PCF fiber core may be hollow or solid. Also the air hole shape, size, relative position, core diameter and nature of the PCF core provides a great design flexibility and hence there are many possible ways to improve its optical properties, such as, confinement loss, birefringence, dispersion, nonlinearity, operating range and number of propagating modes [2–4]. All these parameters indicate a huge possibility in making a new PCF-based sensor technology. These types of sensors may solve the problem in distance monitoring in the industry; mining applications could also use the sensors in hazardous environments, for example high temperature, high pressure, nuclear radiation, noise and high electromagnetic field etc.

This article is a study to represent a compact overview in the prospects of photonic crystal fiber for analyte sensing applications. It consists of a basic theory of PCF, its application, different types of analyte sensors based on its use and variety in design, limitations, existing technology and future scope. The authors also propose an advanced PCF sensing probe with experiment setup and finally some concluding remarks.

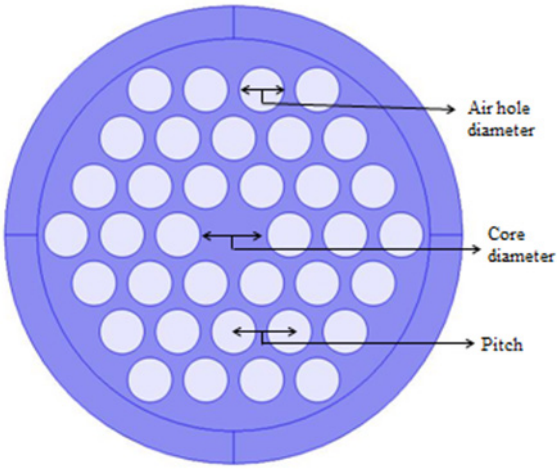

Figure 1. Schematic diagram of PCF and its parameters.

2. Theoretical background of PCF

The working principle of PCF is the same as for photonic crystal. For both of these optical components, incident light gets strongly reflected by a periodic structure. This phenomenon is observable in colorful peacock feathers, the wings of a butterfly and opal in nature. The main concept behind the light propagation through the PCF was that light can be guided in a particular region namely as core, by the arrangement of the 2D photonic crystal around it.

A periodic wavelength scale lattice of micro-structured air holes in glass material working as a photonic crystal around the core is known as cladding. The holey cladding region is running throughout the length of the fiber to prevent leakage of light from the core. Depending on nature of the core, PCF can be broadly classified into two categories, solid core PCF (SC-PCF) and hollow core PCF (HC-PCF) [3–5]. In general, the basic parameters of PCFs are the diameter of the core, the diameter of cladding air holes and the center-to-center distance between two successive air holes, i.e. pitch. A schematic diagram of PCF and its parameters are shown in figure 1. For a PCF, the shape of the core and distribution of cladding air holes provide a great design flexibility as well as enormous improvement in optical properties [4]. For this adaptable nature, PCF-based sensors are considered as an excellent competitor for the currently available conventional sensors based on optical fiber and other commercial sensors.

2.1. Solid core PCFs

The early demonstrated PCF was SC-PCF [3]. In a SC-PCF (figures 2 and 3), the core is made of silica and cladding consists of air holes in a silica background. Though the whole fiber is made of a single material, the holey cladding brings down the refractive index of the cladding in comparison to the core. So, there is a positive refractive index difference

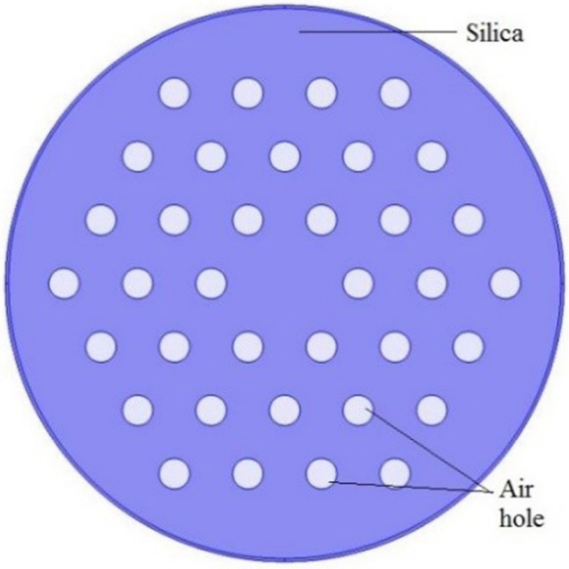

Figure 2. Diagram of a solid core PCF.

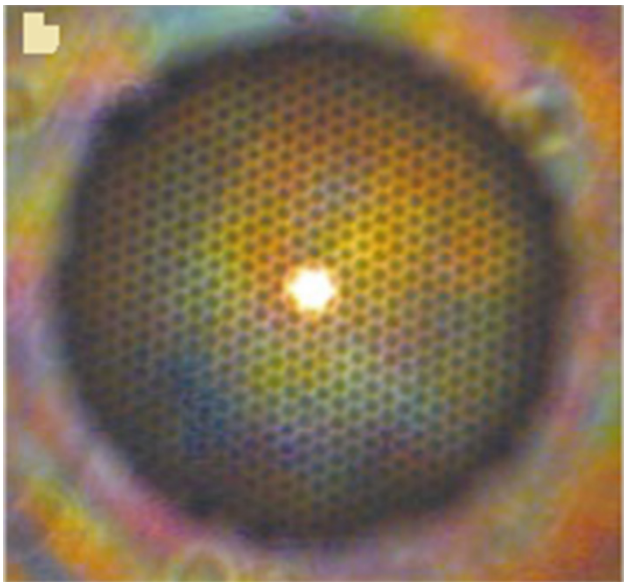

Figure 3. Microscopic picture of a fabricated solid core PCF (reproduced from [4], with the permission of Springer Nature).

between core and cladding. Based on this, light is guided in the core by a modified total internal reflection (TIR) [4].

SC-PCFs have many advanced optical properties, such as endlessly single-mode propagation through a long wavelength range [3, 6, 7], high birefringence [8, 9], high nonlinearity [10, 11], large mode area [12, 13], dispersion tailoring [14, 15], and low loss [16, 17] etc. These charming properties make them advantageous, not only in the field of communication [11, 18] but also in supercontinuum generation [19], making Raman fiber laser [20], spectroscopy [21], sensing [22] etc. Numerous SC-PCF-based analyte sensors will be discussed in later sections.

2.2. Hollow core PCFs

In 1999, HC-PCF was reported for the first time [5]. In HC-PCF (figures 4 and 5), the core is made of air and air

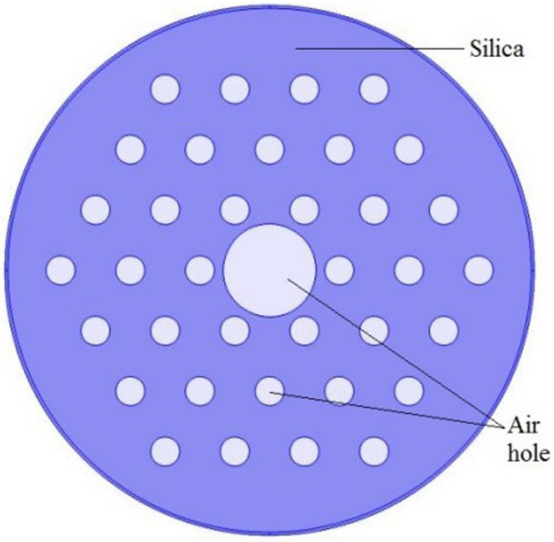

Figure 4. Diagram of a hollow core PCF.

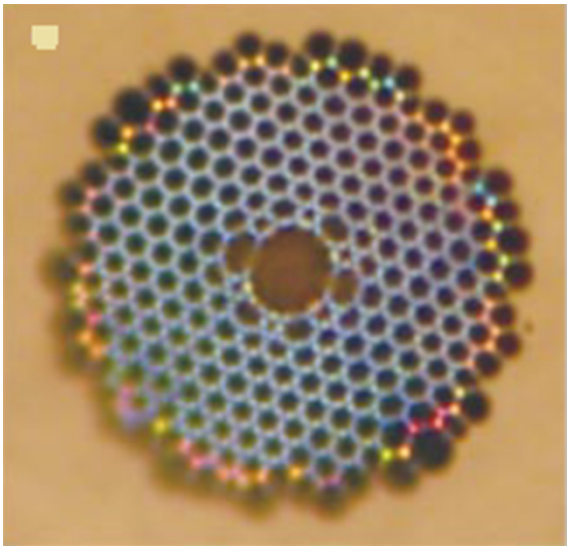

Figure 5. Microscopic picture of fabricated hollow core PCF (reproduced from [4], with the permission of Springer Nature).

holes are distributed around the hollow core in a silica background. Particularly, this surrounding air hole distribution prevents the escape of light from the air core. In a HC-PCF, light is guided in the presence of a photonic band gap (PBG) due to the negative core-cladding refractive index difference. One can correlate the guiding of light through a HC-PCF with the conduction of electrons in a material at the presence of energy-band structure in solid state physics [23].

PBG fiber avoids intrinsic absorption and scattering losses compared to TIR-based fibers. HC-PCF allows the transmission of selective modes depending on the band gap [23]. A HC-PCF is able to support high power density without breakthrough. So, they are capable of pushing the threshold intensity of stimulated Raman scattering and Brillouin scattering up to a high level. The Fresnel reflection problem can be almost eliminated in PBG fiber due to the small refractive index discontinuity between the fiber guided mode and the outer mode. Due to these unique guidance mechanisms this fiber has many

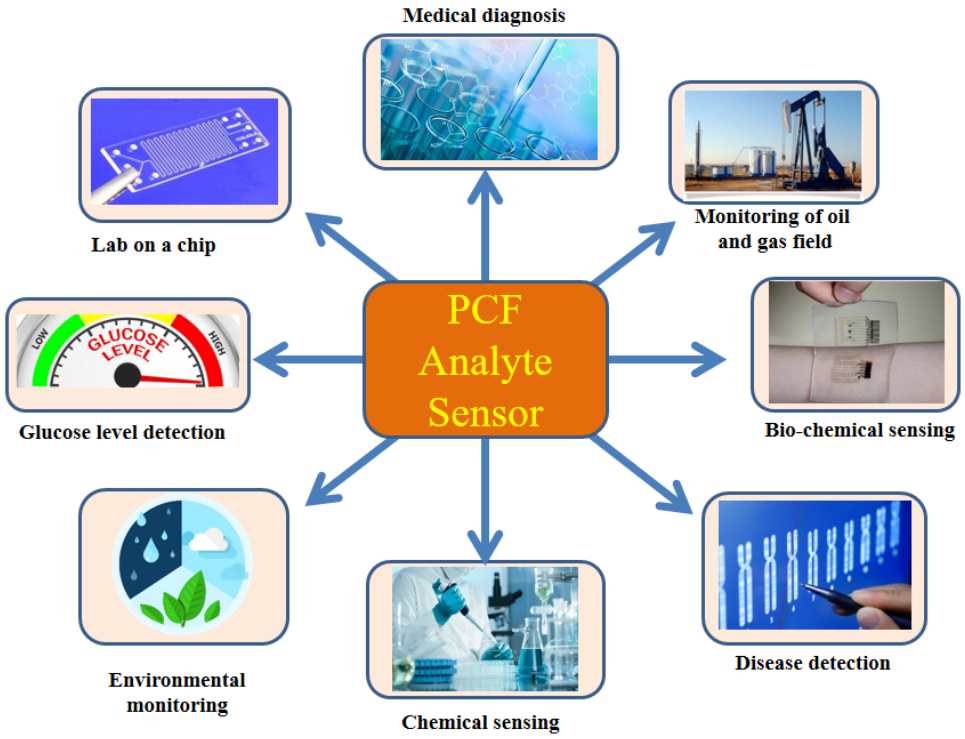

Figure 6. Typical applications of PCF analyte sensors.

pragmatic applications [5, 24–26], such as HC-PCF supports nonlinear optical processes [27, 28], high power ultrafast lasing [29], and optical amplification [30] etc. Gas, low refractive index liquid or vapor can be infiltrated in the core of HC-PCF. It will allow a strong interaction between guided light and an infiltrated analyte. This phenomenon promotes HC-PCF as an efficient element in analyte sensing.

2.3. Numerical formulation

For the guidance of light through PCF, numerical aperture (NA) and V-number are two important parameters. Light gathering potential of an optical fiber is presented by NA. More NA means more light gathering capability of the fiber. It is a dimensionless quantity. For a PCF, NA can be calculated as follows,

$$\mathrm{NA} = \sqrt{n_{\mathrm{core}}^2 - n_{\mathrm{eff}}^2}. \tag{1}$$

Here, n_{core} is the refractive index of core and n_{eff} is the effective refractive index of the guided mode of PCF. n_{eff} can be presented as $n_{\mathrm{eff}} = \beta/k_0$; where β is the propagation constant of guided mode and k_0 is free space propagation constant. Also, $k_0 = 2\pi/\lambda$; λ is the propagating wavelength [31].

V-number clearly indicates the endlessly single mode (ESM) propagation capability of a PCF. When a PCF is able to accommodate only fundamental mode throughout a very long wavelength range then it is known as an endlessly single mode fiber. For a PCF refractive index difference between core and cladding is directly dependent on propagating wavelength. According to Mortensen *et al* [6], the V-number of a PCF can be calculated as

$$V_{\mathrm{PCF}}(\lambda) = \frac{2\pi\Lambda}{\lambda}\sqrt{n_{\mathrm{core}}^2(\lambda) - n_{\mathrm{eff}}^2(\lambda)}. \tag{2}$$

Here Λ is pitch of the fiber. It is noticeable that ESM operation of a PCF depends on its structural parameter as well as propagating wavelength. Single mode cut-off criteria for a PCF is $V_{\mathrm{PCF}} < \pi$ [6].

3. PCF analyte sensors

Considering structural flexibility and advanced optical properties, many research groups are showing their interest in making PCF-based sensors. These are going to prove themselves as a strong component in optical device-based sensing field. Versatile application fields of these sensors are presented in figure 6. At the beginning, efforts were mainly focused in making sensors using commercially available PCFs. In most of the cases, PCFs were integrated with different interference techniques, such as the Sagnac interferometer, core-offset induced interferometer, Mach–Zehnder interferometer and Michelson interferometer [32]. With time, the focus of research was shifted toward the improvement of internal microstructure of PCF to enhance its sensitivity and area of applications. Many PCF-based sensing probes have already been demonstrated using these techniques and applied for sensing different parameters. Scientists are still trying to improve the techniques for making highly sensitive commercially available PCF-based sensors. This article is an endeavor towards giving a brief overview of the development of PCF-based analyte sensors. Based on the measuring entity, these sensors are classified and discussed in the proceeding sections.

3.1. Refractive index sensors

In many situations, the characterization and *in situ* measurement of fundamental properties of the material are essential.

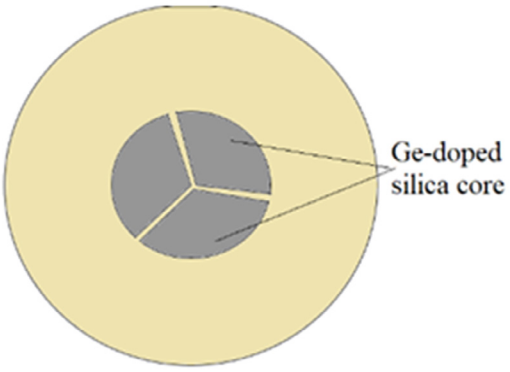

Figure 7. Image of the three-hole PCF with a suspended Ge-doped silica core. It is combined with fiber Bragg grating and holes are filled with analyte then used as a refractive index sensor (reproduced from [38], with the permission of OSA publishing).

To carry out such measurements, optical sensors are a potential which will be compact, lightweight, simply structured, well responsive and immune to electromagnetic interference (EMI). Refractive index (RI) is a fundamental property of any material. For many important applications, RI is necessary to measure, such as in the chemical and food processing industry, fluid industry, measurement of oil concentration in oil industry and quality control of a material. In the beginning of the twenty-first century, fiber Bragg grating (FBG) and conventional optical fiber-based sensors were in use. Diez *et al* demonstrated a gold-coated tapered fiber sensing probe [33]. Swart reported a long period grating (LPG)-based two-path Michelson interferometer for RI sensing [34]. Then, Korposh *et al* demonstrated a poly allylamine hydrochloride (PAH) and SiO_2 nanosphere-coated LPG fiber-based RI sensor [35]. Oliveira *et al* presented a multi-parameter sensing probe that consisted of one untapered FBG, one tapered FBG and one no-core fiber section [36]. During this time, various PCF-based sensors have started to develop, which are having high sensitivity and long sensing range.

At the earlier stage, mostly large mode area (LMA) PCF-based sensors were reported. In 2005 Minkovich *et al* [37] demonstrated a LMA tapered fiber sensor, which consisted of a cladding air hole collapsed region. It has the resolution of around 1×10^{-5} RIU for RI higher than 1.44. Then a sensing probe was fabricated [38] in which a three-hole microstructured optical fiber was combined with a standard FBG that is written in the suspended Ge-doped silica core. It has a resolution of 3×10^{-5} and 6×10^{-5} RIU around mean refractive indices 1.33 and 1.40 respectively (figure 7). An infiltrated photonic band gap fiber-based RI sensor [39] was demonstrated having resolution of 2×10^{-6} RIU in the RI range from 1.333 to 1.390. It works based on a demodulation technique and has a blue shift of 110 nm for RI change of 0.02 at RI 1.35 (figure 8). Then, a 32 mm long interferometer was fabricated [40] that consists of a sensing probe made of a LMA PCF spliced between two SMFs. Using this, RI was measured from the shift of interference pattern with changing analytes. It has a resolution of 2.9×10^{-4} in the RI range from 1.38 to1.44. In the same period, a liquid infiltration technique successfully combined with PCF, due to its hollow nature and

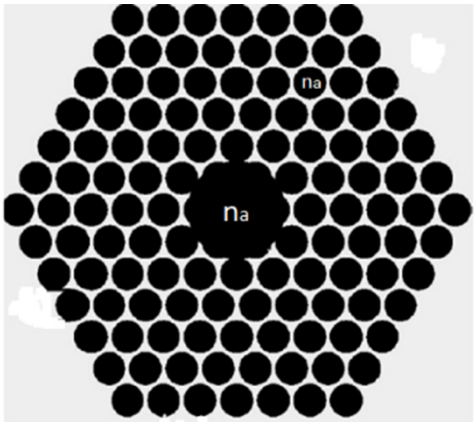

Figure 8. Schematic diagram of the photonic band gap fiber with a hollow core. It is filled with a tested analyte (n_a) for refractive index measurement (reproduced from [39], with the permission of Elsevier publishing).

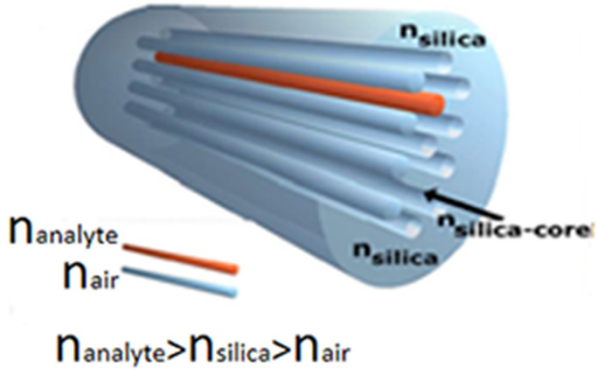

Figure 9. Diagram of an analyte channel solid core PCF containing a microfluidic channel (red colored) worked as a refractive index sensing probe (reproduced from [41], with the permission of OSA publishing).

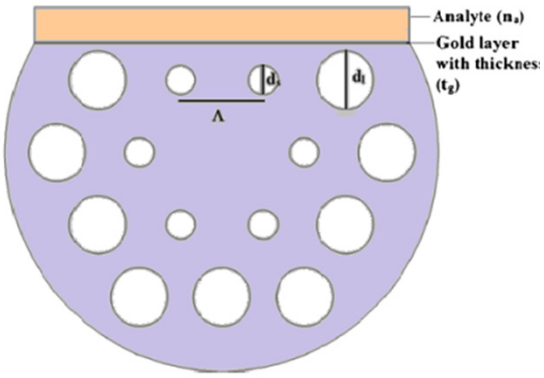

Figure 10. Cross section of the proposed gold layer containing D-shaped PCF refractive index sensing probe which worked based on SPR theory (reproduced from [45], with the permission of Springer publishing).

many improvised RI sensors, were demonstrated. Using this technique, a single cladding air hole infiltrated SC-PCF [41] sensor was reported for RI sensing. It worked based on strong field overlap between the core mode and fluid infiltrated waveguide associated mode. This sensor has a high sensitivity of 30 100 nm RIU^{-1} with a resolution of 4.6×10^{-7} (figure 9).

Table 1. Comparative representation of different PCF-based RI sensors.

Reported structure	Spectral range (nm)	RI Range	Observed quantity	Sensitivity	Resolution(RIU)	Ref.
Photonic crystal fiber modal interferometer	1250–1340	1.33–1.45	Interference pattern shift	—	7×10^{-5}	[48]
Coated photonic band gap fibers	~1550	1.33–1.35	Wavelength	2.2×10^{4} nm RIU^{-1}	~10^{-6}	[49]
Surface long-period gratings deposited onto a D-shaped photonic crystal fiber	1250–1650	1.00–1.45	Wavelength	585.3 nm RIU^{-1}	—	[50]
Cavity made with a micro-mirror and a bi-functional large radius of curvature lensed PCF	1260–1350	1.328–1.357	Intensity	—	2.60×10^{-5}	[51]
PCF-based polymer fiber directional coupler	400–900	1.337–1.344	Wavelength	1.66×10^{3} nm RIU^{-1}	~2×10^{-6}	[52]
Selectively liquid infiltrated dual core PCF	1200–1700	1.30–1.40	Wavelength	65 166 nm RIU^{-1}	—	[53]
Four-analyte channel PCF consisting two gold wire	1600–2000	1.30–1.79	Wavelength	3233 nm RIU^{-1}	3.09×10^{-5}	[54]
Metamaterial-incorporated D shaped PCF	755–830	1.34–1.36	Wavelength	3700 nm RIU^{-1}	2.70×10^{-5}	[55]
PCF consisting of an annular analyte channel and gold-graphene layer coating	700–1000	1.38–1.42	Wavelength	7500 nm RIU^{-1}	1.33×10^{-5}	[56]
Gold-coated D-shaped PCF with various side polished lengths	500–1200	1.40–1.42	Wavelength	7381 nm RIU^{-1}	—	[57]
Diamond ring fiber coated with gold layer from inside and directly filled with an analyte	500–900	1.33–1.39	Wavelength	6000 nm RIU^{-1}	1.67×10^{-5}	[58]
Gold nanowire combined with solid core PCF	600–1100	1.27–1.36	Wavelength	2350 nm RIU^{-1}	2.80×10^{-5}	[59]
Gold grating incorporated D-shaped PCF	1500–1700	1.36–1.38	Wavelength	3340 nm RIU^{-1}	5.98×10^{-6}	[60]
Silver nano grating incorporated dual core PCF	550–850	1.330–1.365	Wavelength	13 600 nm RIU^{-1}	7.35×10^{-6}	[61]
Alcohol filled LMA-10 PCF-based Mach–Zehnder interferometer	1524–1572	1.335–1.350	Wavelength	386 nm RIU^{-1}	—	[62]

Then dual core PCF was introduced in the field of sensing. An RI sensor [42] was proposed based on all solid band gap guided dual core PCFs in which coupling between the core modes is modified by the liquid infiltrated central hole. It shows a sensitivity of 7000 nm RIU^{-1} in a relatively large RI range.

The sensitivity of PCF sensors was increased in many folds when the plasmonic layer was incorporated internally or externally with the fiber structure. The number of publication is increased with the PCF-based SPR sensors. The sensitivity of SPR-based sensors can be determined from wavelength, amplitude or phase interrogation method. A selectively silver film-coated PCF sensor [43] was demonstrated by Zhang *et al*. An externally graphene and silver-coated PCF sensor [44] was reported with external flow of the analyte having sensitivity 860 RIU^{-1} with a high resolution of 4×10^{-5} RIU. Then a D-shaped PCF-based SPR sensor was presented [45] which has a very high sensitivity 7700 nm RIU^{-1} and a resolution of 1.30×10^{-5} RIU in the RI range from 1.43 to 1.46 (figure 10). In 2016 Rifat *et al* proposed a unique multi-core flat fiber SPR sensor for high RI sensing [46]. It showed maximum wavelength sensitivity 23 000 nm RIU^{-1} and amplitude sensitivity 820 RIU^{-1} with a high resolution in the RI range 1.460–1.475. Very recently a D-shaped PCF sensing probe is reported which consists a curved gold layer and two light passing passageways near the polished surface [47]. It is giving high sensitivity of 11 055 nm RIU^{-1} with a resolution of 9.05×10^{-6} RIU for low RI monitoring. A few more RI sensors are presented in table 1.

3.2. Gas sensors

Optical fiber-based gas sensing techniques are getting popular with time over the use of spectrophotometers in analyzing the spectrum of gases and to identify them. The atmosphere consists of many gases, some of which are essential for leaving where as some are harmful. The levels of essential gases should be maintained and the levels of harmful gases should be controlled under a safety limit. Leakage or emission of hydrocarbons, hydrogen and various toxic gases from industry, thermal power stations, mines, home, workplace, motor vehicles, chemical plants are serious matters of concern for the safety of living things as well as controlling environmental pollution. In this regard, the development of gas sensing technology is thrust into the context of global sustainable development. In the present situation, it is necessary to develop a gas sensor that is less power consuming, lightweight, fast responding, having a long lifetime and able to work in extremely hazardous environments. To fulfill these criteria in last few decades many fiber-based gas sensors and remote sensing systems are reported. Low loss silica fiber consisting of a gas sensor [63] is one of them. Cao *et al* demonstrated a plastic clad optical fiber-based sensing probe for an evanescent wave using gas sensing [64]. Also a LPG fiber coated

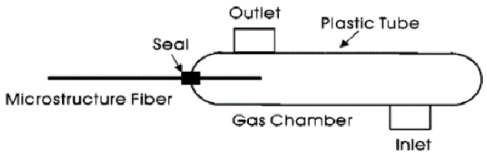

Figure 11. Silica-air microstructure fiber incorporated gas chamber used for evanescent wave gas detection (reproduced from [69], with the permission of SPIE publishing).

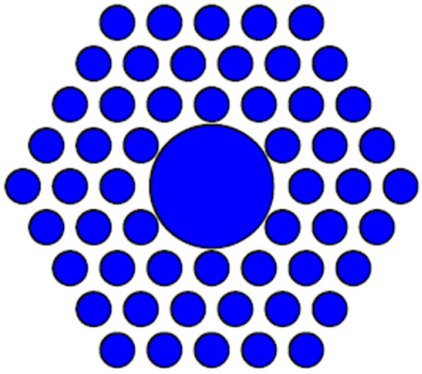

Figure 12. Fibers with a seven-hole adjoined triangular-lattice geometry which was used for evanescent wave-based aqueous sensing applications (reproduced from [71], with the permission of IOP science publishing).

with a metal-oxide-semiconductor film was presented as a gas sensor [65]. Then a silver layer as well as a vapor sensitive polymer layer consistent fiber-based Fabry–Pérot (FP) cavity was applied for gas sensing by Liu *et al* [66]. Alali *et al* reported a fiber loop ring down based gas flow sensor [67]. But less versatility in structure and material restrained development of ultrasensitive gas sensors.

PCF-based gas sensors are new hope in this field. Though this is not a fully developed technology, it has many possibilities. Also this technology is very compatible with telecommunication systems, so they are suitable for real time detection and remote sensing [68]. According to our best knowledge, in 2002 for the first time a SC-PCF-based gas sensor [69] was demonstrated using an evanescent-wave sensing technique (figure 11). The next year, a PCF gas sensor was demonstrated [70] for acetylene and methane sensing having relative sensitivity 12.6% and 14.9% respectively. It has a response time of ~1 min. Then a water core microstructure fiber consisting of a seven-hole adjoined triangular-lattice (SAT) geometry was designed [71] for gas sensing. It works based on band gap theory and having loss less than 1 dB m^{-1} (figure 12). A stretched air hole containing a modified microstructure optical fiber sensor was proposed [72]. It is working based on evanescent wave sensing and having maximum relative sensitivity of 30%–35% with low loss (figure 13). Both SC-PCF and HC-PCF can be used in making gas sensors, however due to the more interaction of the guided light with suspected gases HC-PCFs are more preferred. From a reported article it can be clearly visualized that a PCF having an air hole at the center of the core shows much better relative sensitivity. Also, sensitivity suffers increment with an increasing central air hole diameter [73]. Then hollow core photonic band gap fibers

Figure 13. A stretched air hole based modified microstructure optical fiber working on evanescent wave-based sensor (reproduced from [72], with the permission of Elsevier publishing).

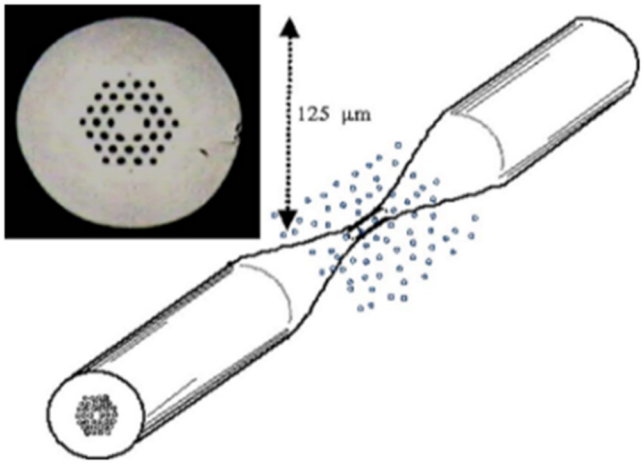

Figure 14. SEM image of PCF with micro tapper PCF exposed to vapor molecules of volatile compounds for gas molecule detection (reproduced from [76], with the permission of AIP Publishing).

were presented [74, 75] at a different bandwidth for high concentration methane sensing. A three air hole ring consisting of a tapered SC-PCF sensor was reported [76] for gas molecule detection (figure 14).

At the same time a photonic band gap fiber was combined with the spontaneous gas-phase Raman scattering [77] for a natural gas density measurement based on photomultiplier. A microstructure optical fiber Bragg grating was presented [78] as a gas sensor working based on reflection mode. It has a sensitivity of ~0.017–0.022 dB/%. Also a C-type fiber and a Ge-doped ring defect PCF was combined together [79] for making an in-line chemical gas sensor. In this device, a sensing probe was connected to the light source and detector using SMF. In this probe, PCF works as a sensing medium and C-type fibers as inlet or outlet components. This sensor works in a low concentration of ~ 0.5% with a fast dynamic response time at a low pressure of 10 Torr (figure 15).

A Raman spectroscopy-based HC-PCF was proposed [80] as a sensor, which is capable of measuring various gases and chemical vapors at very low concentration. Later on an index-guiding PCF consisting of a hollow high index (GeO_2–SiO_2) ring with a central air hole as well as five layers of air holes

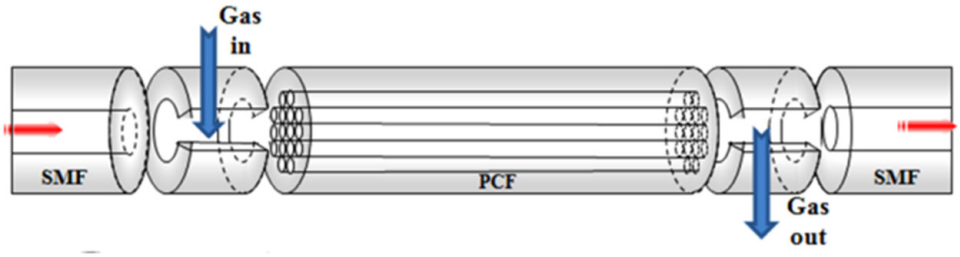

Figure 15. Structure of the proposed gas sensor device. Here PCF is used as the sensing medium, c-type fibers as inlet/outlet components for gases and SMF for the connection to the source and detector (reproduced from [79], with the permission of OSA publishing).

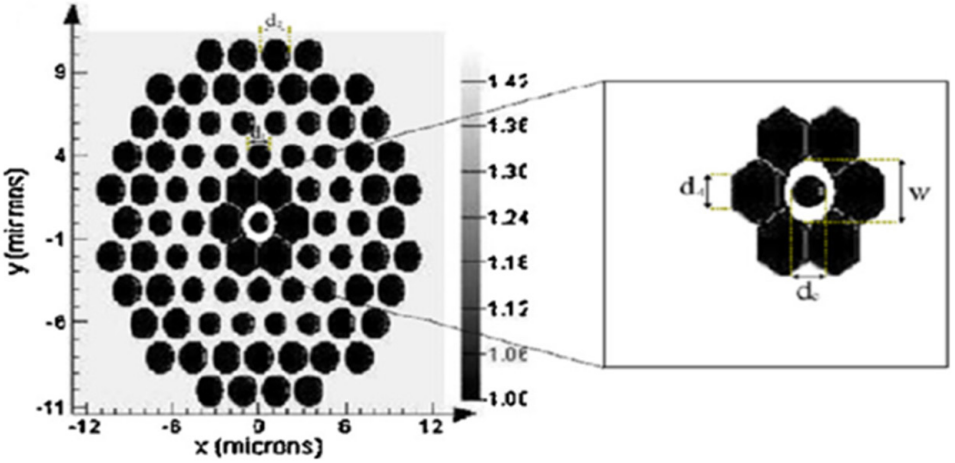

Figure 16. Hexagonal holes consisting of a proposed PCF structure used for flammable and/or toxic gas sensing (reproduced from [81], with the permission of Elsevier publishing).

in cladding was reported [81] as a gas sensor. It has relative sensitivity 13.23% for methane at a 1.33 μm wavelength with a confinement loss of 3.77×10^{-6} dB m^{-1} (figure 16). A lightweight SC-PCF (LMA-8) consisting of an in-line interferometer was demonstrated [82] for hydrogen concentration measurement from 0% to 5%. It shows sensitivity of 0.25 nm for one presence of hydrogen using reflection technique. A suspended ring-core PCF-based in-line gas sensor was experimentally demonstrated [83] for acetylene detection. In this sensor, a suspended ring-core fiber is combined with a c-type fiber and MMF. It shows much higher sensitivity in comparison to the conventional PCF sensors. Then a grapefruit PCF internally coated with a micro porous hybrid polymer of poly (ally amine)-co-poly(ethylene glycol) (PAH/PEG) thin film was demonstrated [84] for 2,4-dinitrotoluene vapor sensing. It has sensitivity of 2 pm/ppb_v at a vapor pressure 411 ppb_v and temperature of 25 °C (figure 17). Recently a graphene-coated tapered PCF MZI is reported [85] for hydrogen sulphide gas sensing having sensitivity of 0.031 43 nm ppm^{-1} in the range of 0–45 ppm.

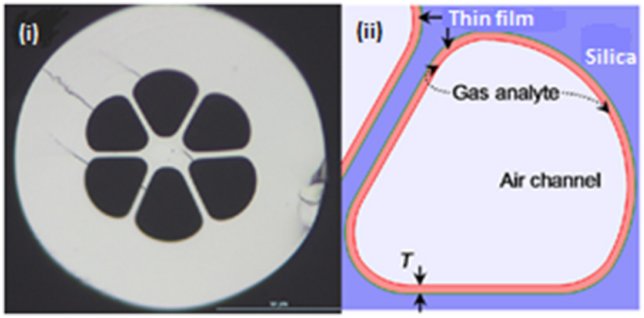

Figure 17. (i) SEM image of grapefruit PCF and (ii) the inner side is coated with specific gas-sensitive thin film. Long period grating is combined with this fiber and used as a gas sensor (reproduced from [84], with the permission of SPIE publishing).

3.3. Bio sensors

PCF-based bio sensors are a point of interest of many research groups due to its great potential in versatile applications, such as, health monitoring, chemical analysis, medicine preparation, pharmaceutical testing, defense, and food technology. Silica-based optical fibers have good bio-compatibility [86]; so these fiber sensors are considered as a good competitor of available commercial bio sensors. Also, fiber sensors can be sterilized without affecting their properties. PCF-based sensors are nonelectrical so they can be used safely in medical diagnosis. Due to the holey nature of PCF, bio-chemical samples can be accommodated in holes of fiber in liquid or gaseous form, and as a result interaction between the guided light and suspected analytes is very high. So, using this, characteristics of high sensitivity as well as portable sensing probes can be manufactured. Only a few nano liter or micro liter analyte samples are needed to use a PCF sensor. Though fiber-based tip sensors needed a very small amount of analyte [87, 88] it is not the case for many

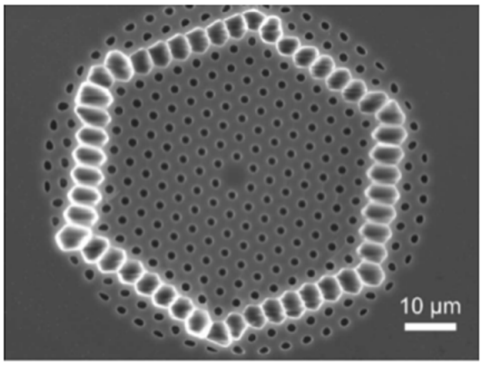

Figure 18. SEM image of a double-clad PCF used for bio sensing (reproduced from [89], with the permission of OSA publishing).

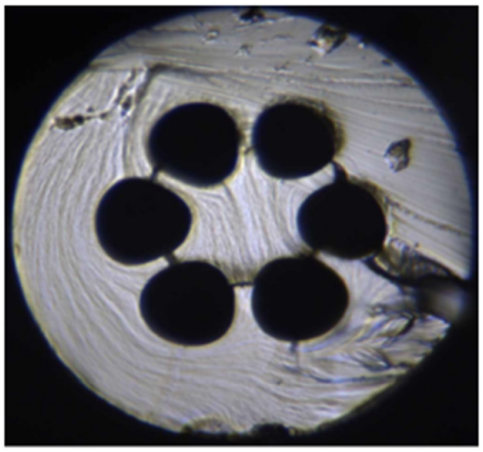

Figure 19. Micrograph of the end-face of the microstructured polymer optical fiber used as a biosensor (reproduced from [90], with the permission of OSA publishing).

conventional sensors. All these unique features make the PCF using bio sensors suitable for present time practice with a lot of future hopes. During the development of PCF-based bio-chemical sensors two trends can be clearly visualized. The focus was shifted from the structural design to the combination of SPR phenomenon with PCF for the development of advanced bio sensors.

In 2003 a double-clad PCF bio sensor was demonstrated [89] for two-photon fluorescence detection using dye material (figure 18). Jensen *et al* reported a DNA detectable 20 cm long air-suspended PCF sensing probe [22]. Then a micro structured polymer optical fiber (mPOF) based antibody sensor was demonstrated [90] which contains six air holes in the core region and antibodies are captured inside of these holes. For this structure, bridges are supporting the core during cleaving. The outer diameter and air hole diameter of this mPOF are 300 μm and 60 μm respectively; the microscopic image is shown in figure 19. Sometimes water molecule detection becomes necessary in the bio-medical field. Keeping this in mind, a sensor was reported [91] using a HC-PCF having a core diameter of ~50 μm. Raman resonance technique was combined with the fiber to identify the stretching vibrations of water molecules. Then a PCF-based sensor was demonstrated [92] for low RI bio fluid detection in which both core and cladding are micro structured. It has a sensitivity coefficient of ~4.28 (figure 20).

A long-period grating inscribed LMA-10 PCF was reported for bio layer sensing [93]. The side of the PCF holes are coated with a monolayer of poly-L-lysine (PLL) and DNA. This sensor can be used for double-stranded DNA detection from the resonant wavelength shift with varying layers of thickness. It shows sensitivity of 1.4 nm/1 nm bio layer (figure 21). Cox *et al* demonstrated a kagome lattice cladding consisting of a hollow core microstructured optical fiber (HC-MOF)-based rhodamine sensor [94]. It works based on the surface enhanced Raman scattering (SERS) phenomenon and silver nanoparticles are used as a rhodamine absorber (figure 22). In the same year, a soft glass microstructured optical fiber-based protein concentration measurement sensor was reported [95] having three air holes at the center.

In 2007 a HC-PCF-based dye concentration detection sensor was reported [96], which is able to measure down to 1×10^{-10} M (figure 23). Then a polymethyl methacrylate (PMMA)-made PCF biosensor was proposed [97]. It consists of an immobilized antigen sensing layer on inner walls of holes. It is able to perform label-free bio sensing of selective antibody biomolecules with sensitivity up to 20 nm/1 nm bio layer. Also, a silica-made exposed core fiber had been fabricated [98] and applied for biochemical sensing (figure 24). Emiliyanov *et al* demonstrated a TOPAS cyclic olefin copolymer made of an mPOF [99] biosensor. It is able to detect selective antibodies, such as Cy3-labelled α-streptavidin and Cy5-labelled α-CRP.

Sensitivity as well as the sensing range of PCF sensors are improvised considerably when plasmonic metal layers are incorporated with the fiber structure. In this way, an index-guided PCF sensing probe working based on surface-enhanced Raman scattering (SERS) was reported [100]. It consists of four big air holes in the core region. Also, gold nanoparticles are associated with this probe either by coating inner walls of air holes or by mixing with the filled analyte. For both of the cases, probes are quite sensitive. When gold nano particle coating is applied then it is able to measure 10^{-5} M rhodamine B solution and for the gold analyte mixture infiltration it is able to measure 10^{-7} M rhodamine B solution (figure 25). A broad spectral SERS-based sensor was developed [101] using silver nanoparticle cluster-incorporated SC-PCF. The silver nanoparticle cluster is synthesized using the green synthesis process. It is able to measure 4-Mercaptobenzoic acid down to 10^{-6} M (figure 26). Recently Rifat *et al* proposed [102] a very high sensitive titanium di-oxide and the gold-coated D-shaped bio-sensor having sensitivity 46 000 nm RIU^{-1} and resolution 2.2×10^{-6}. In 2017, a quasi-D-shaped PCF using a plasmonic biosensor was proposed by An *et al.* The polished surface of this sensor was coated with graphene and indium tin oxide. It has maximum wavelength sensitivity 10 693 nm RIU^{-1} and resolution 9.35×10^{-6} RIU in the

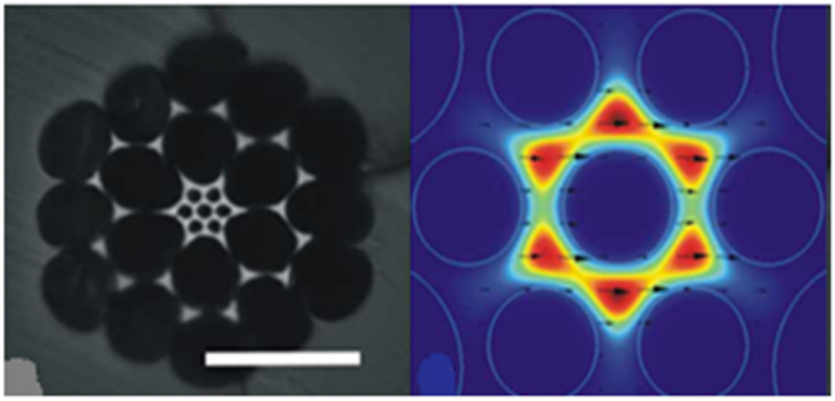

Figure 20. Polymer (PMMA) microstructured fiber. Fabricated microstructured fiber and an electrical field profile. It is usable for low refractive index liquid bio-molecule sample sensing (reproduced from [92], with the permission of OSA publishing).

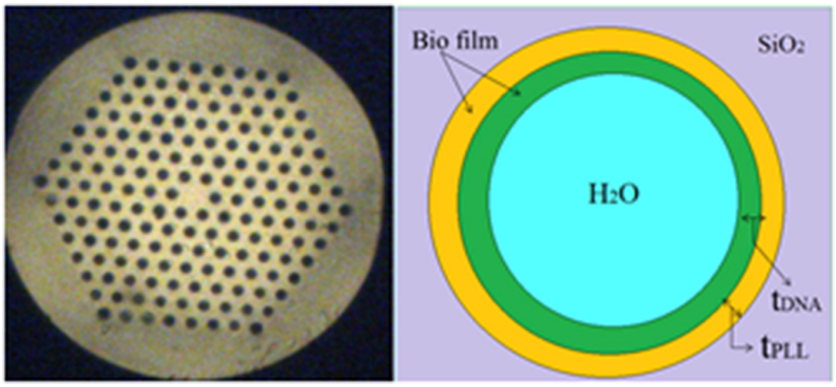

Figure 21. End facet of the LMA10 PCF and a hole of this PCF containing biofilm. The combination of this PCF with a long period of grating is usable for the thickness measurement of the monolayer of poly-L-lysine (PLL) and double-stranded DNA bio-layer (reproduced from [93], with the permission of OSA publishing).

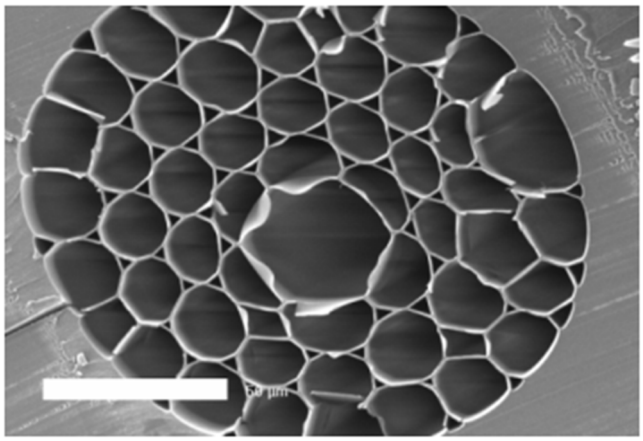

Figure 22. SEM image of the hollow core microstructured optical fiber with a kagome lattice cladding was used for rhodamine detection based on a surface enhanced resonant Raman scattering technique (reproduced from [94], with the permission of OSA publishing).

analyte RI range from 1.33 to 1.38 [103]. Based on the position of incorporated plasmonic metal layer SPR sensors can be classified into two categories, such as internally metal film-coated and externally metal film-coated sensing probes. A few more SPR-based bio sensors having versatile structures are presented in table 2.

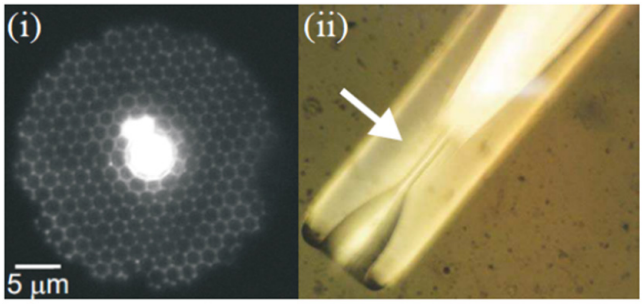

Figure 23. (i) Selectively filled hollow core PCF, and (ii) a microscope image of it after the cladding holes have been sealed by a fusion splicer. The arrow showing the section where the analyte can be filled in the existing hollow core. It was used for bio sample detection (reproduced from [96], with the permission of OSA publishing).

3.4. Humidity sensors

Humidity measurement is inherent in the case of environmental monitoring, air conditioning, food processing, horticulture, and structural monitoring in greenhouses, museums, humidors, and industrial space etc. PCF-based humidity sensors are able to satisfy all these purposes. Mathew *et al* demonstrated a PCF-consisting interferometer [114] using a humidity sensor having a sensitivity of-24 pm/%RH for relative humidity (RH) greater than 70%. This sensor was fabricated without

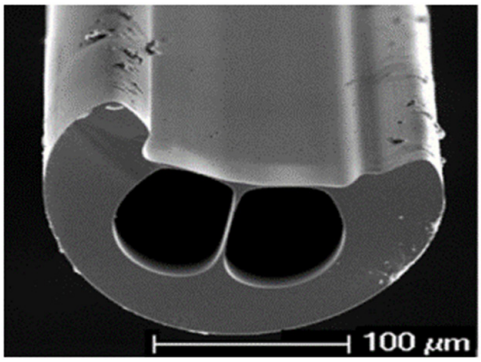

Figure 24. Exposed-core silica-made fiber used for bio-chemical sensing applications (reproduced from [98], with the permission of OSA publishing).

any hygroscopic material and works based on reflection mode, shown in figure 36. A polymer-infiltrated PCF-based interferometer was designed [115] by splicing an SMF and a LMA-10 fiber to study RH. This sensor has a compact size, less response time, measurement accuracy, long-term stability and less thermal sensitivity. These advanced features make it suitable for measuring RH ranging from 86% to 98% with high resolution. In the same year, Noor *et al* demonstrated a hollow core photonic band gap fiber (HC-PBF)-based sensing head [116] without any humidity detectable material coating. There is a small gap between HC-PBF and connecting SMF to satisfy air diffusion into HC-PBF. Over the range of 0 to 90% RH it shows a sensitivity of 3.02 mV/1% RH with good linear response. The effect of agarose coating thickness on the sensitivity of a RH sensor [117] was studied by the same group. The sensing probe was made of a PCF-SMF spliced element using an interferometer and shows high sensitivity of 1100 pm/% RH for an RH range of 90%–98%.

A polyvinyl alcohol-coated PCF modal interferometer-based RH sensor was demonstrated [118] having a sensitivity of 40.9 pm/%RH within a range of 20%–95% RH. Then a SMF-PCF-SMF spliced probe consisting of an interferometer sensor was reported [119] without any thin film coating. This fast responding sensor gives the highest sensitivity of 188.3 pm/%RH in the range of 80%–95% RH (figure 37). In 2013, a RH sensor head is demonstrated [120] based on a hybrid fiber probe. This device is composed of a FBG and agarose infiltrated reflection type PCF interferometer. It shows a sensitivity of 0.163 dB/%RH in an RH range of 60%–95%. In the same period, an interior nano-film-coated PCF-LPG-based humidity sensor was reported [121]. Figure 38 shows the microscopic image of the interior polyallylamine hydrochloride and polyacrylic acid-coated PCF. Figure 38(ii) shows LPG inscribed in PCF by focusing a CO_2 laser beam with a galvanometer and the inset consists of the outlook of the PCF-LPG probe. This sensor has an RH sensitivity of 0.0007 %/pm.m. A SMF-PCF-SMF spliced probe was applied for humidity measurement [122]. Poly allylamine hydrochloride (PAH) and poly acrylic acid (PAA) polymeric nano-coatings were deposited layer-by-layer on this fiber probe. This humidity sensor has a sensitivity of 0.86 mrad/% RH for 20%–95% RH with a response time of 0.3 s (figure 39). Then a

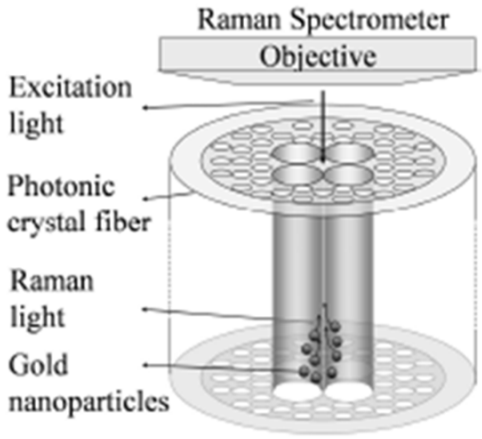

Figure 25. Schematic of the rhodamine sensing probe. It consists of an index-guided PCF having four big air holes and gold nanoparticles for the generation of surface enhanced Raman scattering (reproduced from [100], with the permission of OSA publishing).

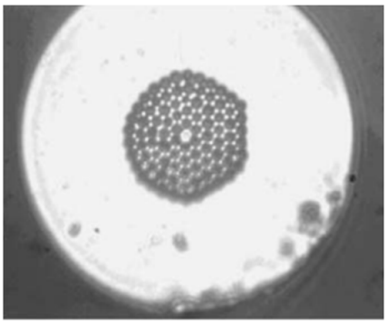

Figure 26. Microscopic image of the cross-section of the solid core holey PCF used for mercaptobenzoic acid detection (reproduced from [101], with the permission of Springer publishing).

SnO_2 nano film-coated PCF-based humidity sensor was demonstrated [123] which is able to measure 20 to 90% RH with a resolution of 0.067% HR.

3.5. Other types of sensors

There are few more unique PCF analyte sensors. Wu *et al* demonstrated a polyimide-coated Hi-Bi PCF-based Sagnac interferometer for salinity measurement [124] having a sensitivity of 0.742 nm $(mol/l)^{-1}$. The radial pressure effect on this spiral probe is induced by the swelling of the polyimide coating. In 2018, a dual core PCF-based salinity sensor [125] was proposed with a sensitivity of 5675 nm RIU^{-1} and detection limit of 0.0037 RIU. Earlier, SERS was generated using metal nanoparticles and applied for bio imaging, medical diagnosis, and bio-sensing etc [126, 127]. A few years before, a SERS active HC-PCF probe was demonstrated [128] for detecting serological liver cancer biomarkers, epidermal growth factor receptor biomarkers and oral squamous carcinoma cell lysates using three different SERS nano tags. It is also able to identify hepatocellular carcinoma biomarkers-alpha fetoprotein and alpha-1-antitrypsin secreted in the supernatant from Hep3b cancer cell line. In this process, the needed sample volume is ~20 nl (figure 40).

Table 2. Comparative representation of different PCF-based SPR bio sensors.

Proposed structure	Wavelength (nm)	Refractive index range	Observed quantity	Sensitivity	Resolution	Fig.	Ref.
Honeycomb PCF internally coated with a gold layer	940–1060	~1.32	Amplitude wavelength	400/RIU 13 750 nm RIU^{-1}	2.5×10^{-5} RIU 7.2×10^{-6} RIU	27	[104]
Slotted SC-PCF sensor for detection of bio-layer thickness	600–920	1.40–1.42	Amplitude	~0.22/nm	0.044 nm	28	[105]
H-shaped PCF having two U-shaped cavities which are uniformly coated with thin gold and titanium dioxide layer	1450–1650	1.32–1.33	Wavelength	5×10^{3} nm RIU^{-1}	—	29	[106]
Internally gold film coated slotted PCF	500–800	1.33–1.34	Amplitude	220/RIU	4×10^{-5} RIU	—	[107]
External metal nano layers consisting polymer PCF	440–600	1.330–1.335	Amplitude	106/RIU	8.33×10^{-5} RIU	30	[108]
Exposed-core grapefruit fiber with external thin silver coating on the exposed section	880-1200	1.33–1.42	Wavelength	13 500 nm RIU^{-1}	7.41×10^{-5} RIU	31	[109]
Hexagonal PCF externally coated with a copper-graphene layer	520-820	1.33–1.37	Wavelength	2000 nm RIU^{-1}	5×10^{-5} RIU	32	[110]
High birefringent SC-PCF consisting of two big holes internally coated with gold and filled with an analyte	540–660	1.37–1.38	wavelength	3100 nm RIU^{-1}	—	33	[111]
Gold film-coated square-lattice D-shaped PCF	1300–1550	1.34–1.41	wavelength	12 450 nm RIU^{-1}	8.03×10^{-6} RIU	34	[112]
Externally gold layer coated modified hexagonal PCF	590–770	1.33–1.37	Wavelength	1000 nm RIU^{-1}	1×10^{-4} RIU	35	[113]

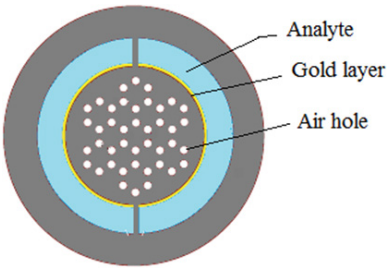

Figure 27. Cross section of solid core PCF having a small central hole surrounding by honeycomb photonic crystal reflector with two large gold-plated channels and an outer aqueous analyte layer as a suspected material (figure courtesy from the [104]).

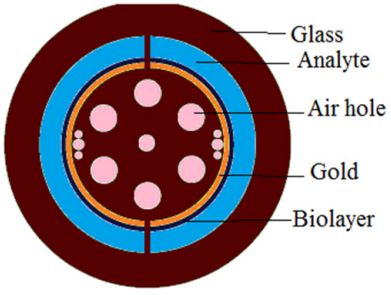

Figure 28. Slotted PCF SPR biosensors consisting of a gold layer with the air hole defects near gold layers. It was used for bio layer thickness measurement (reproduced from [105], with the permission of OSA publishing).

Then a flying particle detector was demonstrated based on a HC-PCF having a core diameter of 12 μm [129]. It works at a 1064 nm wavelength using a long length fiber (figure 41). Johny *et al* proposed a FBG-combined four-ring liquid crystal PCF-based sensor [130]. It was used for oil and gas sensing over a wide wavelength range from 800 to 1700 nm (figure 42). In 2019, a petrol adulteration detection sensor was reported using a dual core PCF probe. It has a sensitivity of 20 161 nm RIU^{-1} with good linear response over a long adulteration range [131].

4. Present technologies and future hopes

Though a PCF-based waveguide was invented in 1996, it took nearly four years to make it applicable as a sensor. The PCF-based sensing technology has enriched a lot theoretically as well as experimentally by the contribution of many research groups. In the present scenario, the majority of the proposed sensors are on paper, i.e. sensor models are proposed based on simulation work. But PCF fabrication technology has been drastically developed in the last decade. It is really hopeful regarding practical realization of those proposed sensors. Earlier PCF was fabricated using the popular stack and draw technique [2] only. After that, many techniques have been developed to fabricate advanced PCFs, such as sol-gel [132], drilling [133], extrusion [134], and 3D printing [135]. Using these techniques, asymmetric PCF structures can also be

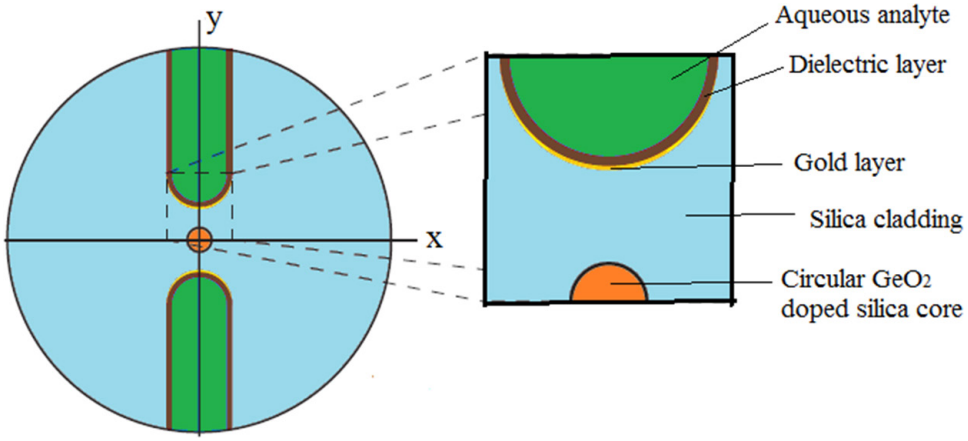

Figure 29. Cross section of the H-shaped fiber sensing probe for analyte sensing. It has a GeO_2 doped solid silica core and two U-shaped analyte channels. The inner surface of these U-shaped regions are covered with a uniform gold and TiO_2 layer successively (figure curtsy from the [106]).

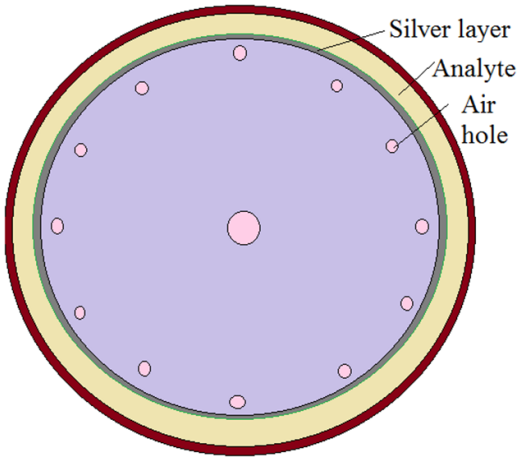

Figure 30. Structure of the large mode area polymer PCF consisting a silver layer surrounded by an analyte channel. It works as a SPR sensor (reproduced from [108], with the permission of MDPI publisher).

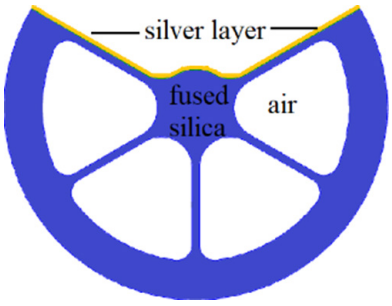

Figure 31. Cross section of the exposed-core grapefruit fiber with silver coating on the exposed section used as an SPR sensor (reproduced from [109], with the permission of MDPI publisher).

realized practically. For the fabrication of PCF sensors generally, a piece of PCF having the length fraction of a centimeter to a few centimeters is spliced between two standard optical fibers to make a sensing probe. Also light can be launched and collect directly from the PCF probe by using free space coupling [136]. Though the commercialization of these sensors are at proposal stage, undoubtedly PCF-based sensors have

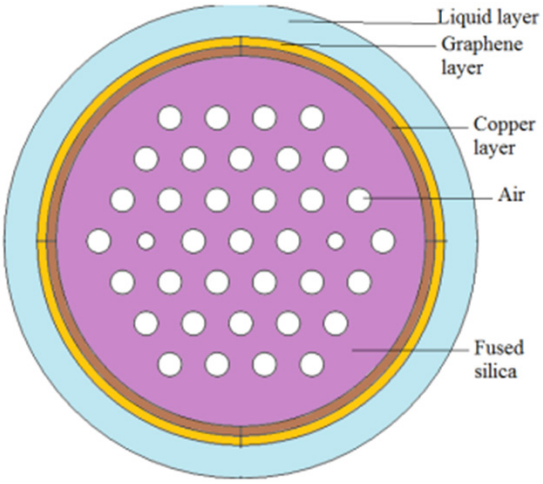

Figure 32. Schematic diagram of the externally copper-graphene-coated PCF with an external analyte channel used for bio-chemical sensing (figure curtsy from the [110]).

huge possibilities over the other available sensors. Moreover, PCF-based sensor fabrication is costly at present but with the development of technology it must be cost effective even to suit the household applications. Currently, PCF-based sensors need some real time applications, improvement of its detection range and the capability of various bio-chemical analyte detection. As such, a geometrical pattern of PCF substantially affects the optical properties of PCF so designing more simple structured PCFs avoiding the structural complexity can take the PCF-based sensor technology to a new height. Advanced PCF sensor technology must be another successful step towards labs on a fiber access. Selective infiltration of PCF micro-channels enhance the interaction between guided light and suspected analytes as well as its sensitivity. Until now, many technological developments take place for the selective infiltration of PCF air holes; such as by applying pressure or by employing capillary forces, using focused ion beam milled micro channels, with the help of dye-doped curable polymers, by blowing a hole through the fiber wall for both air holes of SC-PCF as well as the core of HC-PCF [137–141]. Also, for the fabrication of well responding SPR-based PCF sensors,

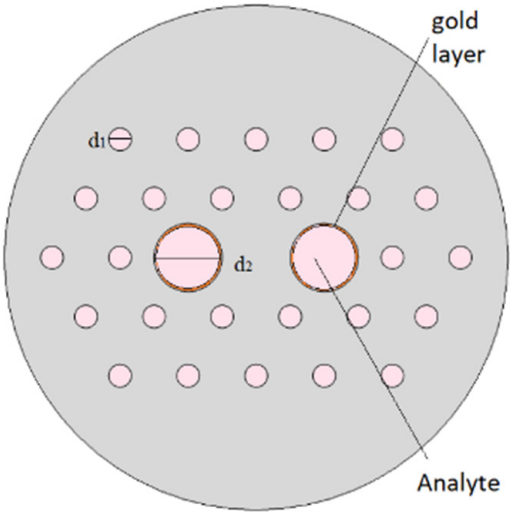

Figure 33. Hi-Bi near-panda microstructured optical fiber with two internal gold-coated analyte filled holes. It was used as an SPR-based biochemical analyte sensor (reproduced from [111], with the permission of IOP science publishing).

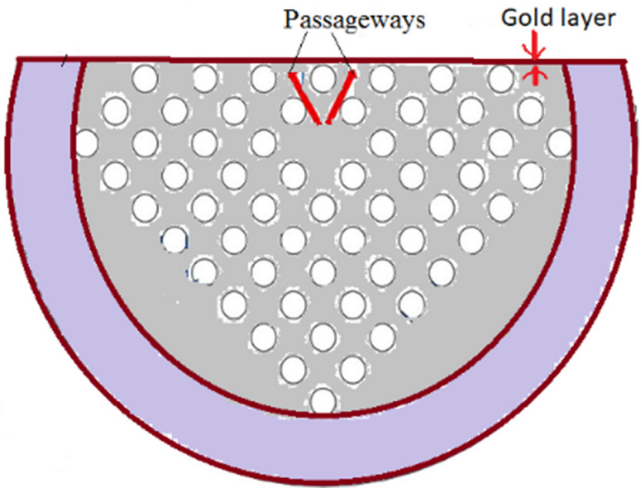

Figure 34. Cross section of the square-coated D-PCF used for biological sensing (reproduced from [112], with the permission -lattice based gold layer of Springer publishing).

uniform plasmonic metal layer coating is needed to reduce surface roughness and make sure there is a streamline flow of the analytes. To ensure uniformity and control the thickness of the plasmonic layer, the chemical vapor deposition technique can be applied [142]. Between these internal and external sensing approaches, later one is more compatible for mass production. So, external sensing using PCF sensors can be promoted more for commercial applications. It will automatically bring down the cost of PCS sensors. Aside from silica, some polymers are also used as the background material of PCFs, for example, TOPAS, poly (methyl methacrylate) (PMMA), polyamide-6 (PA6) etc. These polymer fibers are mainly applied for making sensors working in the THz frequency region [52, 73, 143, 144]. So, these are the starting light of hopes for the PCF sensor technology toward the development of advanced sensors and its significant applications.

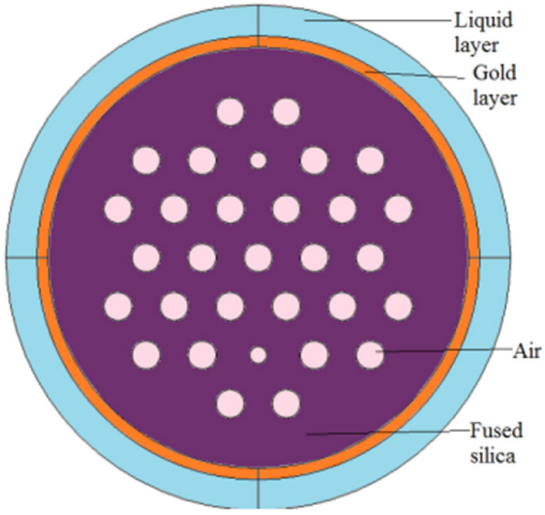

Figure 35. Schematic diagram of the external gold layer-coated PCF SPR sensor used for biological as well as biochemical analyte detection (reproduced from [113], with the permission of Elsevier publishing).

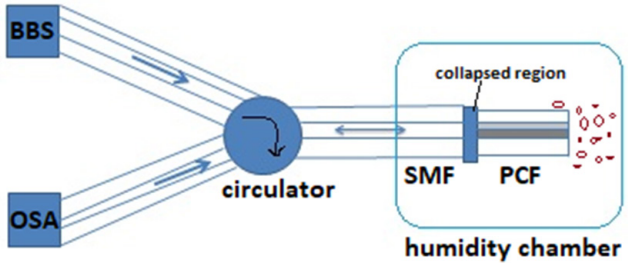

Figure 36. Experimental setup of a PCF interferometer-based relative humidity sensor (reproduced from [114], with the permission of the Institution of Engineering & Technology).

5. Proposal for an advanced PCF sensor

The reduction of PCF sensor manufacture complexity is the biggest challenge in front of researchers. One of these complexities is the air channel filling with analytes and the controlled flow of the analyte through them because the majority of proposed PCF sensors are based on air hole infiltration [145]. An external analyte channel will be a useful solution to this problem. The structural flexibility of PCF can be integrated with the superiority of flat fiber. Flat fibers are advantageous because of their large sensing area, fast response, compatibility with standard optical fiber-based networks, and immunity against EM interference. Over the past few years flat fiber-based waveguides are designed as well as fabricated for communication purposes [146, 147]. Recently, a flat fiber-based multicore analyte sensor was proposed [46] but it is also not free from void infiltration complexity. At the present scenario, doped silica solid cores consisting of flat fiber (figure 43(a)) will be a solution to previous limitations. In this case, a plasmonic metal layer can be deposited on the top surface of the flat fiber by the spattering technique [148] and the suspected analyte can be poured on top of the plasmonic metal. The analyte can be changed without much difficulty as it is situated externally. It is well established that materials,

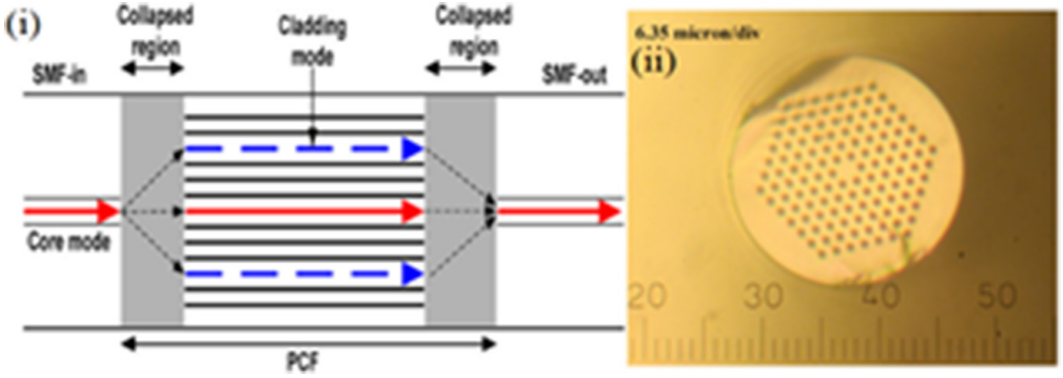

Figure 37. (i) Diagram of the relative humidity sensor consisting of two collapsed regions; (ii) cross section of the PCF used to fabricate this humidity sensor (reproduced from [119], with the permission of IOP science publishing).

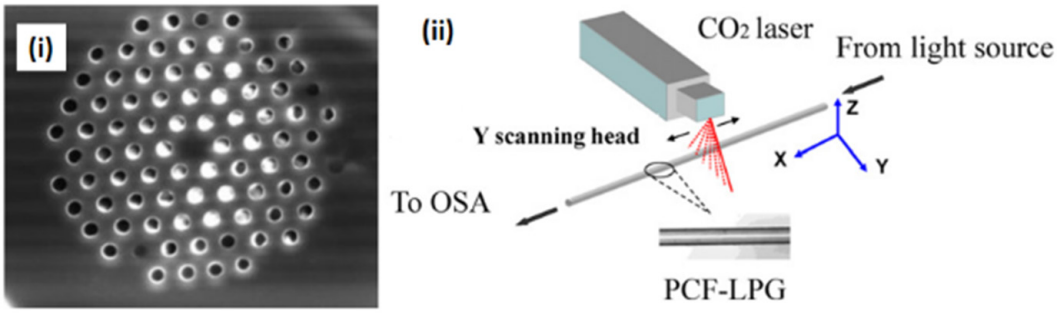

Figure 38. (i) Cross-section of interior nanofilm-coated PCF with polyallylamine hydrochloride and polyacrylic acid. (ii) humidity sensor setup (reproduced from [121], with the permission of Elsevier publishing).

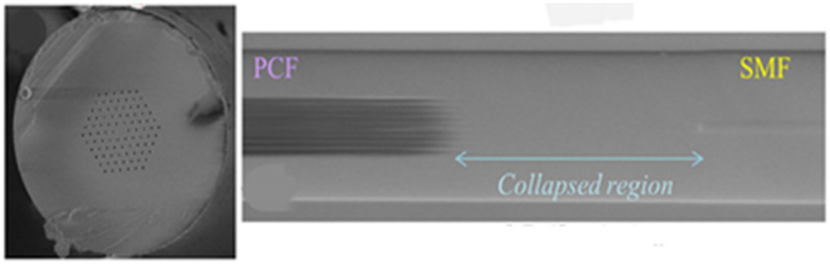

Figure 39. Microscopic image of the PCF-SMF collapsed junction used to build up the interferometer for humidity measurement (reproduced from [122], with the permission of Elsevier publishing).

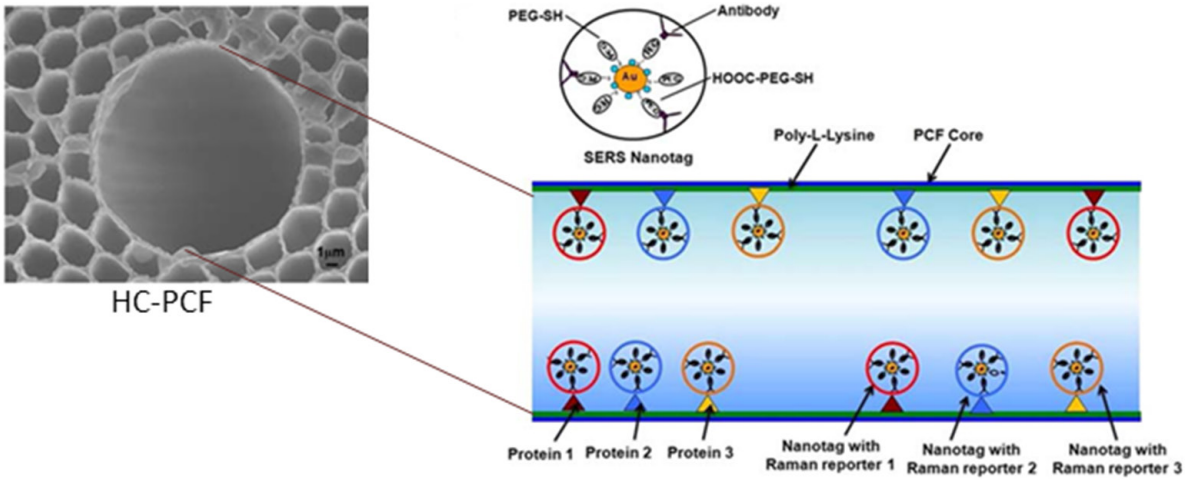

Figure 40. Schematic of the binding of surface-enhanced Raman scattering nano-tags to immobilized biomarkers inside the core of hollow core PCF for multiplex detection (reproduced from [128], with the permission of John Wiley and Sons publishing).

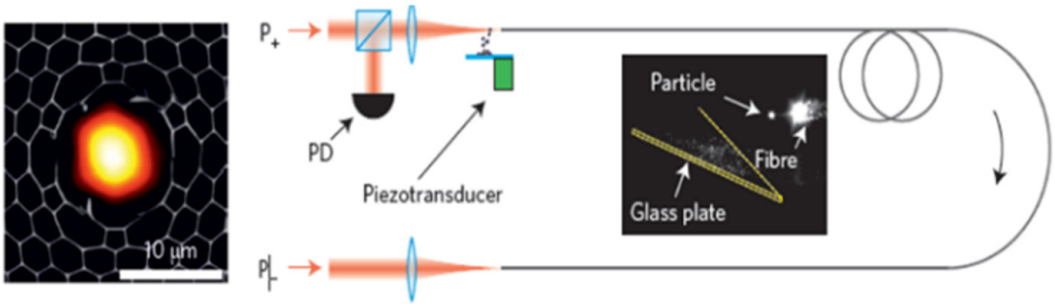

Figure 41. SEM image of the hollow core PCF and experimental setup and with a superimposed near-field optical mode profile at a 1064 nm wavelength (reproduced from [129], with the permission of Springer Nature publishing).

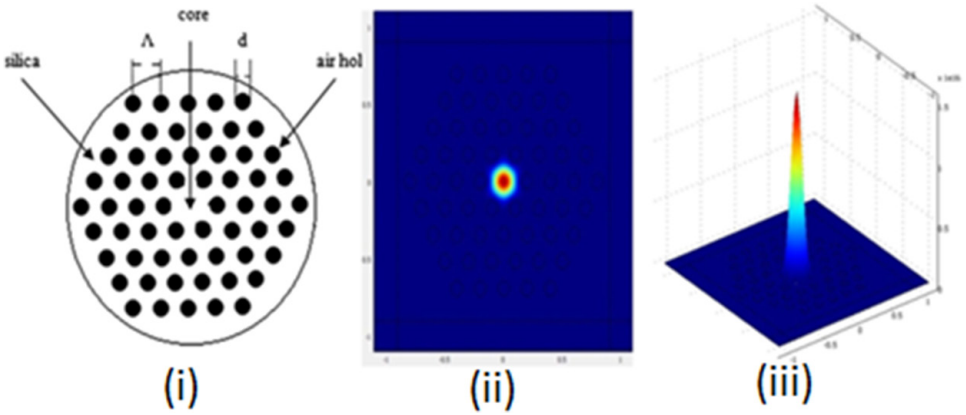

Figure 42. (i) Cross section of liquid crystal PCF with (ii) 2D and (iii) 3D views of electric field pattern for oil and gas sensing (reproduced from [130], with the permission of Springer publishing).

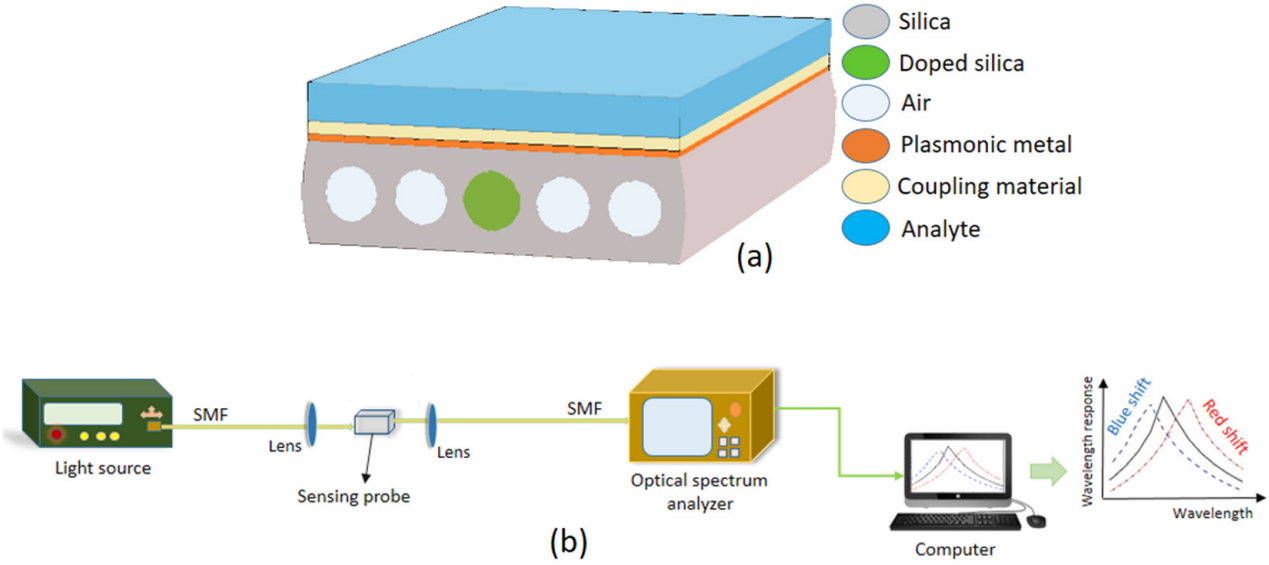

Figure 43. (a) Proposed PCF sensing probe. (b) Schematic of experimental setup.

such as titanium dioxide (TiO_2), graphene-enhance coupling between core guided mode and SPP mode [149, 150]. So, the sensitivity of a flat fiber sensor can be improvised by applying a thin layer of coupling enhancing material in between the plasmonic metal and the analyte. A schematic diagram of the suggested experimental setup using a flat fiber probe is depicted in figure 43(b). Light can be launched from a broad band source to the sensing probe using free space coupling. That can be channelized to the optical spectrum analyzer for SPR spectrum analysis. This proposed sensor can be applied for different liquid chemical sensing.

6. Conclusion

In summary, this article presents an updated review on different types of PCF analyte sensors and its development with time. In the beginning, various analyte sensors were reported using commercially available solid and hollow core PCFs.

Also, most of these sensors work based on interferometry techniques. Later on, the focus of research shifted toward the designing of improvised PCF sensors and their real time applications. This development trend of PCF sensor technology is thoroughly discussed.

The first phase of this write up begins with the theoretical background and basic structures of PCF followed by refractive index sensors, gas sensors, bio sensors, humidity sensors and some other sensors. Variety in PCF structures have tried to be presented based on their applications. It ended up with advantages as well as limitations of PCF sensor technology to date and the proposal of an advanced PCF-based sensor.

Undoubtedly PCF-based sensor technology is a highly potential branch of fiber optics as well as establishes a lot of future potential. PCF fabrication technology is still at its infant stage. There are a few more concerns that have to be overcome, such as its compactness as a sensor device, enhancement of its stability and the increment of its industrial applications.

It can be concluded from the above discussions that variety in the structure of PCF, its usability in different fields and its wide range analyte sensing capability demonstrate its importance for fabricating sensors. The increasing research interest and fast development in this field gives a clear indication about the advancement of PCF sensor technology. It is expecting that, in the near future, PCF sensors will be commercially available even for domestic applications.

ORCID iDs

Moutusi De https://orcid.org/0000-0002-7023-1969

References

[1] Grattan K T V and Sun T 2000 Fiber optic sensor technology: a0.n overview *Sensors Actuators* A **82** 40–61
[2] Russell P 2003 Photonic crystal fibres *Science* **299** 358–62
[3] Knight J C, Birks T A, Russell P S J and Atkin D M 1996 Pure silica single-mode fiber with hexagonal *Opt. Lett.* **21** 1547–9
[4] Knight J C 2003 Photonic crystal fibers *Nature* **424** 847–51
[5] Cregan R F, Mangan B J, Knight J C, Birks T A, Russell P St J, Roberts P J and Allan D C 1999 Single-mode photonic band gap guidance of light in air *Science* **285** 1537–9
[6] Mortensen N A, Folkenberg J R, Nielsen M D and Hansen K P 2003 Modal cut-off and the V-parameter in photonic crystal fibers *Opt. Lett.* **28** 1879–81
[7] Birks T A, Knight J C and Russell P S J 1997 Endlessly single-mode photonic crystal fiber *Opt. Lett.* **22** 961–3
[8] Kuhlmey B, McPhedran R, de Sterke C, Robinson P, Renversez G and Maystre D 2002 Microstructured optical fibers: where's the edge? *Opt. Express* **10** 1285
[9] Knight J C, Wadsworth W J, Arriaga J, Mangan B J, Birks T A and Russell P S J 2000 Highly birefringent photonic crystal fibers *Opt. Lett.* **25** 1325–7
[10] Hansen K P, Jensen J R, Jacobsen C, Simonsen H R, Broeng J, Skovgaard P M W and Peterson A 2002 Highly nonlinear photonic crystal fiber with zero dispersion at 1.55 μm *Optical Fiber Commun. Conf. and Exhibit*
[11] Hansen K P 2003 Dispersion flattened hybrid-core nonlinear photonic crystal fiber *Opt. Express* **11** 1503–9
[12] Kristiansen R E, Hansen K P, Broeng J, Skovgaard P M W, Nielsen M D, Petersson A, Hansen T P, Mangan B, Jakobsen C and Simonsen H R 2005 Microstructured fibers and their applications *Proc. ReuniònEspañola de Optoelectrònica Optoel* (Elche, Spain) pp 13–5
[13] Knight J C, Birks T A, Cregan R F, Russell P S J and de Sandro P D 1998 Large mode area photonic crystal fiber *Electron. Lett.* **34** 1347–8
[14] Reeves W H, Knight J C, Russell P St J and Roberts P J 2002 Demonstration of ultra-flattened dispersion in photonic crystal fibers *Opt. Express* **10** 609–13
[15] Ferrando A, Silvestre E, Miret J J and Andrés P 2000 Nearly zero ultra flattened dispersion in photonic crystal fibers *Opt. Lett.* **25** 790–2
[16] Kurokawa K, Tajima K, Tsujikawa K and Nakajima K 2005 Reducing the losses in photonic crystal fibers *Proc. European Conf. on Optical Commun.* (Glasgow, Scotland) pp 25–29
[17] Roberts P J *et al* 2005 Ultimate low loss of hollow-core photonic crystal fibers *Opt. Express* **13** 236–44
[18] Ju J, Jin W and Demokan M S 2003 Properties of a highly birefringent photonic crystal fiber *IEEE Photonics Technol. Lett.* **15** 1375–7
[19] Wadsworth W J, Blanch A O, Knight J C, Birks T A, Martin Man T-P and Russell P S 2002 Supercontinuum generation in photonic crystal fibers and optical fiber tapers: a novel light source *J. Opt. Soc. Am.* B **19** 2148–55
[20] Pinto A M R, Frazão O, Santos J L and Lopez-Amo M 2011 Multiwavelength Raman fiber lasers using Hi–Bi photonic crystal fiber loop mirrors combined with random cavities *J. Lightwave Technol.* **29** 1482–1488
[21] Holzwarth R, Udem T, Hänsch T W, Knight J C, Wadsworth W J and Russell P S 2000 Optical frequency synthesizer for precision spectroscopy *Phys. Rev. Lett.* **85** 2264–7
[22] Jensen J B *et al* 2004 Photonic crystal fiber based evanescent-wave sensor for detection of biomolecules in aqueous solutions *Opt. Lett.* **29** 1974–6
[23] Smith C M, Venkataraman N, Gallagher M T, Müller D, West J A, Borrelli N F, Allan D C and Koch K W 2003 Low-loss hollow-core silica/air photonic bandgap fibre *Nature* **424** 657–9
[24] Couny F, Benabid F and Light P S 2006 Large pitch kagome-structured hollow-core photonic crystal fiber *Opt. Lett.* **31** 3574–6
[25] Wang Y Y, Wheeler N V, Couny F, Roberts P J and Benabid F 2011 Low loss broadband transmission in hypocycloid-core Kagome hollow-core photonic crystal fiber *Opt. Lett.* **36** 669–71
[26] Russell P S J 2006 Photonic-crystal fibers *J. Lightwave Technol.* **24** 4729–49
[27] Ghosh S, Sharping J E, Ouzounov D G and Gaeta A L 2005 Resonant optical interactions with molecules confined in photonic band-gap fibers *Phys. Rev. Lett.* **94** 093902–1
[28] Dudley J M and Roy Taylor J 2009 Ten years of nonlinear optics in photonic crystal fiber *Nat. Photon.* **3** 85–90
[29] Saraceno C, Emaury F, Diebold A, Schriber C, Debord B, Gerome F, Südmeyer T, Benabid F and Keller U 2005 Hollow-core photonic crystal fibers for high-power, ultrafast lasers *SPIE Newsroom* (https://doi.org/10.1117/2.1201503.005818)
[30] Guichard F *et al* 2015 Nonlinear compression of high energy fiber amplifier pulses in air-filled hypocycloid-core Kagome fiber *Opt. Express* **23** 7416
[31] Crisp J and Barry E 2005 *Introduction to Fiber Optics* (Oxford: Elsevier)
[32] Pinto A M R and Lopez-Amo M 2012 Photonic crystal fibers for sensing applications *J. Sens.* **2012** 1–21

[33] Diez A, Andres M V and Cruz J L 2001 In-line fiber-optic sensors based on the excitation of surface plasma modes in metal-coated tapered fibers *Sens. Actuators* B **73** 95–9

[34] Swart P L 2004 Long-period grating Michelson refractometric sensor *Meas. Sci. Technol.* **15** 1576–80

[35] Korposh S, Lee S W, James S W and Tatam R P 2011 Refractive index sensitivity of fibre-optic long period gratings coated with SiO_2 nanoparticle mesoporous thin films *Meas. Sci. Technol.* **22** 075208

[36] Oliveira R, Osório J H, Aristilde S, Bilro L, Nogueira R N and Cordeiro C M B 2016 Simultaneous measurement of strain, temperature and refractive index based on multimode interference, fiber tapering and fiber Bragg gratings *Meas. Sci. Technol.* **27** 075107

[37] Minkovich V, Villatoro J, Monzón-Hernández D, Calixto S, Sotsky A and Sotskaya L 2005 Holey fiber tapers with resonance transmission for high-resolution refractive index sensing *Opt. Express* **13** 7609–14

[38] Phan Huy M C, Laffont G, Dewynter V, Ferdinand P, Roy P, Auguste J-L, Pagnoux D, Blanc W and Dussardier B 2007 Three-hole microstructured optical fiber for efficient fiber Bragg grating refractometer *Opt. Lett.* **32** 2390–2

[39] Sun J and Chan C C 2007 Photonic bandgap fiber for refractive index measurement *Sens. Actuators* B **128** 46–50

[40] Jha R, Villatoro J, Badenes G and Pruneri V 2009 Refractometry based on a photonic crystal fiber interferometer *Opt. Lett.* **34** 617

[41] Wu D K C, Kuhlmey B T and Eggleton B J 2009 Ultrasensitive photonic crystal fiber refractive index sensor *Opt. Lett.* **34** 322–4

[42] Wu Y, Town G E and Bang O 2010 Refractive index sensing in an all-solid twin-core photonic bandgap fiber *IEEE Sens. J.* **10** 1192

[43] Zhang X, Wang R, Cox F M, Kuhlmey K and Large M C 2007 Selective coating of holes in microstructured optical fiber and its application to in-fiber absorptive polarizers *Opt. Express* **15** 16270–8

[44] Dash J N and Jha R 2014 Graphene-based birefringent photonic crystal fiber sensor using surface plasmon resonance *IEEE Photonics Technol. Lett.* **26** 1092–5

[45] Gangwar R K and Singh V K 2017 Highly sensitive surface plasmon resonance based d-shaped photonic crystal fiber refractive index sensor *Plasmonics* **12** 1367–72

[46] Rifat A A, Mahdiraji G A, Sua Y M, Ahmed R, Shee Y G and Adikan F R M 2016 Highly sensitive multi-core flat fiber surface plasmon resonance refractive index sensor *Opt. Express* **24** 2485

[47] Chen X, Xia L and Li C 2018 Surface plasmon resonance sensor based on a novel D-shaped photonic crystal fiber for low refractive index detection *IEEE Photonics J.* **10** 6800709

[48] Jha R, Villatoro J and Badenes G 2008 Ultrastable in reflection photonic crystal fiber modal interferometer for accurate refractive index sensing *Appl. Phys. Lett.* **93** 2006–9

[49] Kuhlmey B T, Coen S and Mahmoodian S 2009 Coated photonic bandgap fibres for low-index sensing applications: cutoff analysis *Opt. Express* **17** 16306–21

[50] Kim H J, Kown O J, Lee S B and Han Y G 2011 Measurement of temperature and refractive index based on surface long-period gratings deposited onto a D-shaped photonic crystal fiber *Appl. Phys.* B **102** 81–5

[51] Mudhana G, Seob Park K, Ryu S Y and Lee B H 2011 Fiber-optic probe based on a bifunctional lensed photonic crystal fiber for refractive index measurements of liquids *IEEE Sens. J.* **11** 1178–83

[52] Lee K J, Liu X, Vuillemin N, Lwin R, Leon-Saval S G, Argyros A and Kuhlmey B T 2014 Refractive index sensor based on a polymer fiber directional coupler for low index sensing *Opt. Express* **22** 17497

[53] Gangwar R K and Singh V K 2015 Refractive index sensor based on selectively liquid infiltrated dual core photonic crystal fibers *Photonics Nanostruct.—Fundam. Appl.* **15** 46–52

[54] An G, Li S, Yan X, Zhang X, Yuan Z, Wang H, Zhang Y, Hao X, Shao Y and Han Z 2017 Extra-broad photonic crystal fiber refractive index sensor based on surface plasmon resonance *Plasmonics* **12** 465–71

[55] Santos D F, Guerreiro A and Baptista J M 2017 SPR optimization using metamaterials in a D-type PCF refractive index sensor *Opt. Fiber Technol.* **33** 83–8

[56] Liu C, Yang L, Su W, Wang F, Sun T, Liu Q, Mu H and Chu P K 2017 Numerical analysis of a photonic crystal fiber based on a surface plasmon resonance sensor with an annular analyte channel *Opt. Commun.* **382** 162–1

[57] Xie Q, Chen Y, Li X, Yin Z, Wang L, Geng Y and Hong X 2017 Characteristics of D-shaped photonic crystal fiber surface plasmon resonance sensors with different side-polished lengths *Appl. Opt.* **56** 1550–5

[58] Ng W L, Rifat A A, Wong W R, Mahdiraji G A and Mahamd Adikan F R 2018 A novel diamond ring fiber-based surface plasmon resonance sensor *Plasmonics* **13** 1165–70

[59] Liu C, Yang L, Liu Q, Wang F, Sun Z and Sun T 2017 Analysis of a surface plasmon resonance probe based on photonic crystal fibers for low refractive index detection *Plasmonics* **13** 779–84

[60] Lu J, Li Y, Han Y, Liu Y and Gao J 2018 D-shaped photonic crystal fiber plasmonic refractive index sensor based on gold grating *Appl. Opt.* **57** 5268–72

[61] Jiao S, Gu S, Yang H, Fang H and Xu S 2018 Highly sensitive dual-core photonic crystal fiber based on a surface plasmon resonance sensor with a silver nano-continuous grating *Appl. Opt.* **57** 8350–8

[62] Zhang Y, Luo Y, Peng B, Fan R, Wu Q and Ren Z 2019 Novel optical fiber refractive sensor fabricated with an alcohol-filled photonic crystal fiber based on a Mach–Zehnder interferometer *Opt. Fiber Technol.* **48** 278–82

[63] Chan K, Ito H and Inaba H 1984 An optical-fiber-based gas sensor for remote absorption measurement of low-level CH_4 gas in the near-infrared region *J. Lightwave Technol.* **2** 234–7

[64] Cao W and Duan Y 2005 Optical fiber-based evanescent ammonia sensor *Sens. Actuators* B **110** 252–9

[65] Gu Z and Xu Y 2007 Design optimization of a long-period fiber grating with sol-gel coating for a gas sensor *Meas. Sci. Technol.* **18** 3530–6

[66] Liu J, Sun Y and Fan X 2009 Highly versatile fiber-based optical Fabry–Pérot gas sensor *Opt. Express* **17** 2731–8

[67] Alali H and Wang C 2014 Fiber loop ringdown gas flow sensors *Meas. Sci. Technol.* **25**

[68] Carvalho J P, Lehmann H, Bartelt H, Magalh F, Ferreira L A, Knight J C, Santos J L, Van Roosbroeck J and Ara F M 2009 Remote system for detection of low-levels of methane based on photonic crystal fibres and wavelength modulation spectroscopy *J. Sens.* **2009** 398403

[69] Hoo Y L, Jin W, Ho H L and Wang D N 2002 Evanescent-wave gas sensing using microstructure fiber *Opt. Eng.* **41** 8–9

[70] Hoo Y L, Jin W, Shi C, Ho H L, Wang D N and Ruan S C 2003 Design and modeling of a photonic crystal fiber gas sensor *Appl. Opt.* **42** 3509–15

[71] John M Fini 2004 Microstructure fibres for optical sensing in gases and liquids *Meas. Sci. Technol.* **15** 1120–8

[72] Ho H L, Hoo Y L, Jin W, Ju J, Wang D N, Windeler R S and Li Q 2007 Optimizing microstructured optical fibers for evanescent wave gas sensing *Sens. Actuators* B **122** 289–94

[73] Ã Z Z, Fang-di Z, Min Z and Pei-da Y 2008 Gas sensing properties of index-guided PCF with air-core *Opt. Laser Technol.* **40** 167–74

[74] Cubillas A M, Lazaro J M, Conde O M and Petrovich M N 2008 Methane sensing at 1300 nm band with hollow-core photonic bandgap fibre as gas cell *Electron. Lett.* **44** 403–4

[75] Gayraud N, Kornaszewski Ł W, Stone J M, Knight J C, Reid D T, Hand D P and Macpherson W N 2008 Mid-infrared gas sensing using a photonic bandgap fiber *Appl. Opt.* **47** 1269–77

[76] Minkovich V P, Villatoro J, Kreuzer M P, Badenes G, Minkovich V P, Villatoro J and Kreuzer M P 2008 Photonic crystal fiber microtaper supporting two selective higher-order modes with high sensitivity to gas molecules Photonic crystal fiber microtaper supporting two selective higher-order modes with high sensitivity to gas molecules *Appl. Phys. Lett.* **93** 081106

[77] Buric M P, Chen K P, Falk J and Woodruff S D 2008 Enhanced spontaneous Raman scattering and gas composition analysis using a photonic crystal fiber *Appl. Opt.* **47** 4255–61

[78] Yan G, Zhang A P, Ma G, Wang B, Kim B and Im J 2011 Fiber-optic acetylene gas sensor based on microstructured optical fiber Bragg GRATINGS *IEEE Photonics Technol. Lett.* **23** 1588–90

[79] Kassani S H, Park J, Jung Y, Kobelke J and Oh K 2013 Fast response in-line gas sensor using C-type fiber and Ge-doped ring defect photonic crystal fiber *Opt. Express* **21** 14074

[80] Yang X, Chang A S P, Chen B, Gu C and Bond T C 2013 Sensors and actuators B: chemical High sensitivity gas sensing by Raman spectroscopy in photonic crystal fiber *Sens. Actuators* B **176** 64–8

[81] Olyaee S, Naraghi A and Ahmadi V 2014 Optik High sensitivity evanescent-field gas sensor based on modified photonic crystal fiber for gas condensate and air pollution monitoring *Optik* **125** 596–600

[82] Zhou F, Qiu S-J, Luo W, Xu F and Lu Y-Q 2014 An all-fiber reflective hydrogen sensor based on a photonic crystal fiber in-line interferometer *IEEE Sens. J.* **14** 1133–6

[83] Kassani S H, Khazaeinezhad R, Jung Y, Kobelke J K and Oh K 2015 Suspended ring-core photonic crystal fiber gas sensor with high sensitivity and fast response suspended ring-core photonic crystal *IEEE Photonics J.* **7** 2700409

[84] Tao C 2016 Grapefruit photonic crystal fiber sensor for gas sensing application *Opt. Eng.* **55** 057103

[85] Feng X, Feng W, Tao C, Deng D, Qin X and Chen R 2017 Hydrogen sulfide gas sensor based on graphene-coated tapered photonic crystal fiber interferometer *Sens. Actuators* B **247** 540–5

[86] Giannetti A, Barucci A, Cosi F, Pelli S, Tombelli S, Trono C and Baldini F 2015 Optical fiber nanotips coated with molecular beacons for DNA detection *Sensors* **15** 9666–80

[87] Zhang Y, Dhawan A and Vo-Dinh T 2011 Design and fabrication of fiber-optic nanoprobes for optical sensing *Nanoscale Res. Lett.* **6**

[88] Barucci A, Cosi F, Giannetti A, Pelli S, Griffini D, Insinna M, Salvadori S, Tiribilli B and Righini G C 2015 Optical fibre nanotips fabricated by a dynamic chemical etching for sensing applications *J. Appl. Phys.* **117** 053104

[89] Myaing M T, Ye J Y, Norris T B, Thomas T, Baker J R, Wadsworth W J, Bouwmans G, Knight J C and Russell P S J 2003 Enhanced two-photon biosensing with double-clad photonic crystal fibers *Opt. Lett.* **28** 1224–6

[90] Jensen J B, Hoiby P E, Emiliyanov G, Bang O, Pedersen L H and Bjarklev A 2005 Selective detection of antibodies in microstructured polymer optical fibers *Opt. Express* **13** 5883

[91] Konorov S O, Fedotov A B, Zheltikov A M and Miles R B 2005 Phase-matched four-wave mixing and sensing of water molecules by coherent anti-Stokes Raman scattering in large-core-area hollow photonic-crystal fibers *J. Opt. Soc. Am.* B **22** 2049

[92] Cordeiro C M B, Franco M A R, Chesini G, Barretto E C S, Lwin R, Brito Cruz C H and Large M C J 2006 Microstructured-core optical fibre for evanescent sensing applications *Opt. Express* **14** 13056

[93] Rindorf L, Jensen J B, Dufva M, Pedersen L H, Høiby P E and Bang O 2006 Photonic crystal fiber long-period gratings for biochemical sensing *Opt. Express* **14** 8224–31

[94] Cox F M, Argyros A, Large M C J and Kalluri S 2007 Surface enhanced Raman scattering in a hollow core microstructured optical fiber *Opt. Express* **15** 13675–81

[95] Ruan Y, Schartner E P, Ebendorff-Heidepriem H, Hoffmann P and Monro T M 2007 Detection of quantum-dot labelled proteins using soft glass microstructured optical fibers *Opt. Express* **15** 17819

[96] Smolka S, Barth M and Benson O 2007 Highly efficient fluorescence sensing with hollow core photonic crystal fibers *Opt. Express* **15** 12783–91

[97] Markos C, Yuan W, Vlachos K, Town G E and Bang O 2011 Label-free biosensing with high sensitivity in dual-core microstructured polymer optical fibers *Opt. Express* **19** 7790

[98] Kostecki R, Ebendorff-Heidepriem H, Davis C, McAdam G, Warren-Smith S C and Monro T M 2012 Silica exposed-core microstructured optical fibers *Opt. Mater. Express* **2** 1538

[99] Emiliyanov G, Høiby P E, Pedersen L H and Bang O 2013 Selective serial multi-antibody biosensing with TOPAS microstructured polymer optical fibers *Sensors* **13** 3242–51

[100] Yan H, Liu J, Yang C, Jin G, Gu C and Hou L 2008 Novel index-guided photonic crystal fiber surface-enhanced Raman scattering probe *Opt. Express* **16** 8300–5

[101] Xie Z, Lu Y, Wei H, Yan J, Wang P and Ming H 2009 Broad spectral photonic crystal fiber surface enhanced Raman scattering probe *Appl. Phys.* B **95** 751–5

[102] Rifat A A, Ahmed R, Mahdiraji G A and Adikan F R M 2017 Highly sensitive D-shaped photonic crystal fiber-based plasmonic biosensor in visible to near-IR *IEEE Sens. J.* **17** 2776–83

[103] An G, Li S, Wang H and Zhang X 2017 Metal oxide-graphene-based quasi-D-shaped optical fiber plasmonic biosensor *IEEE Photonics J.* **9** 7–12

[104] Gauvreau B, Hassani A, Fassi Fehri M, Kabashin A and Skorobogatiy M A 2007 Photonic bandgap fiber-based surface plasmon resonance sensors *Opt. Express* **15** 11413–26

[105] Hassani A and Skorobogatiy M 2009 Photonic crystal fiber-based plasmonic sensors for the detection of biolayer thickness *J. Opt. Soc. Am.* B **26** 1550

[106] Erdmanis M, Viegas D, Hautakorpi M, Novotny S, Santos J L and Ludvigsen H 2011 Comprehensive numerical analysis of a surface-plasmon-resonance sensor based on an H-shaped optical fiber *Opt. Express* **19** 13980–8

[107] Akowuah E K, Gorman T, Ademgil H, Haxha S, Robinson G K and Oliver J V 2012 Numerical analysis of a photonic crystal fiber based on two polarized modes for biosensing applications *IEEE J. Quantum Electron.* **48** 1403–10

[108] Lu Y, Hao C-J, Wu B-Q, Musideke M, Duan L-C, Wen W-Q and Yao J-Q 2013 Surface plasmon resonance sensor based on polymer photonic crystal fibers with metal nanolayers *Sensors* **13** 956–65

[109] Yang X, Lu Y, Wang M and Yao J 2015 An exposed-core grapefruit fibers based surface plasmon resonance sensor *Sensors* **15** 17106–14

[110] Rifat A A, Mahdiraji G A, Ahmed R, Chow D M, Sua Y M, Shee Y G and Adikan F R M 2016 Copper-graphene-based photonic crystal fiber plasmonic biosensor *IEEE Photonics J.* **8** 4800408

[111] Zhang N M Y, Hu D J J, Shum P P, Wu Z, Li K, Huang T and Wei L 2016 Design and analysis of surface plasmon resonance sensor based on high-birefringent microstructured optical fiber *J. Opt.* **18** 065005
[112] Wang G, Li S, An G, Wang X, Zhao Y, Zhang W and Chen H 2016 Highly sensitive D-shaped photonic crystal fiber biological sensors based on surface plasmon resonance *Opt. Quantum Electron.* **48** 1–9
[113] Rifat A A, Mahdiraji G A, Shee Y G, Shawon M J and Adikan F R M 2016 A novel photonic crystal fiber biosensor using surface plasmon resonance *Procedia Eng.* **140** 1–7
[114] Mathew J, Semenova Y, Rajan G and Farrell G 2010 Humidity sensor based on photonic crystal fibre interferometer *Electron. Lett.* **46** 1341
[115] Mathew J, Semenova Y and Farrell G 2012 Relative humidity sensor based on an agarose-infiltrated photonic crystal fiber interferometer *IEEE J. Sel. Top. Quantum Electron.* **18** 1553–9
[116] Mohd Noor M Y, Khalili N, Skinner I and Peng G D 2012 Optical relative humidity sensor based on a hollow core-photonic bandgap fiber *Meas. Sci. Technol.* **23** 085103
[117] Mathew J, Semenova Y and Farrell G 2013 Effect of coating thickness on the sensitivity of a humidity sensor based on an Agarose coated photonic crystal fiber interferometer *Opt. Express* **21** 842177
[118] Li T, Dong X, Chan C C, Ni K, Zhang S and Shum P P 2013 Humidity sensor with a PVA-coated photonic crystal fiber interferometer *IEEE Sens. J.* **13** 2214–6
[119] Mohd Noor M Y, Kassim N M, Supaat A S M, Ibrahim M H, Azmi A I, Abdullah A S and Peng G D 2013 Temperature-insensitive photonic crystal fiber interferometer for relative humidity sensing without hygroscopic coating *Meas. Sci. Technol.* **24** 105205
[120] Mathew J, Semenova Y and Farrell G 2013 Fiber optic hybrid device for simultaneous measurement of humidity and temperature *IEEE Sens. J.* **13** 1632–6
[121] Zheng S, Zhu Y and Krishnaswamy S 2013 Sensors and Actuators B : Chemical Fiber humidity sensors with high sensitivity and selectivity based on interior nanofilm-coated photonic crystal fiber long-period gratings *Sens. Actuators* B **176** 264–74
[122] Lopez-Torresa D, Elosuaa C, Villatoroc J, Zubiac J, Rothhardte M, Schustere K and Arregui F J 2017 Photonic crystal fiber interferometer coated with a PAH/PAA nanolayer as humidity sensor *Sens. Actuators* B **242** 1065–72
[123] Lopez-Torres D, Elosua C, Villatoro J, Zubia J, Rothhardt M, Schuster K and Arregui F J 2017 Enhancing sensitivity of photonic crystal fiber interferometric humidity sensor by the thickness of SnO_2 thin films *Sens. Actuators* B **251** 1059–67
[124] Wu C, Guan B-O, Lu C and Tam H-Y 2011 Salinity sensor based on polyimide-coated photonic crystal fiber *Opt. Express* **19** 20003–8
[125] Vigneswaran D, Ayyanar N, Sharma M, Sumathi M, Mani Rajan M S and Porsezian K 2018 Salinity sensor using photonic crystal fiber *Sens. Actuators* A **269** 22–8
[126] Vo-dinh T, Yan F and Wabuyele M B 2005 Surface-enhanced Raman scattering for medical diagnostics and biological imaging *J. Raman Spectrosc.* **36** 640–7
[127] Stokes D L, David L and Vo-Dinh T 2000 Development of an integrated single-fiber SERS sensor *Sens. Actuators* B **69** 28–36
[128] Dinish U S, Balasundaram G, Chang Y T and Olivo M 2014 Sensitive multiplex detection of serological liver cancer biomarkers using SERS-active photonic crystal fiber probe *J. Biophotonics* **7** 956–65
[129] Bykov D S, Schmidt O A, Euser T G and Russell P S J 2015 Flying particle sensors in hollow-core photonic crystal fibre *Nat. Photon.* **9** 461–5
[130] Johny J, Prabhu R and Keung W 2016 Investigation of structural parameter dependence of confinement losses in PCF—FBG sensor for oil and gas sensing applications *Opt. Quantum Electron.* **48** 1–9
[131] De M, Pathak A K and Singh V K 2019 Single channel photonic crystal fiber based high sensitive petrol adulteration detection sensor *Optik* **183** 539–46
[132] Bise R T and Trevor D J 2005 Solgel-derived micro-structured fibers: fabrication and characterization *Optical Fiber Commun. Conf.* **3** 3
[133] Zhang P, Zhang J, Yang P, Dai S, Wang X and Zhang W 2015 Fabrication of chalcogenide glass photonic crystal fibers with mechanical drilling *Opt. Fiber Technol.* **26** 176–9
[134] Ghazanfari A, Li W, Leu M C and Hilmas G E 2017 A novel freeform extrusion fabrication process for producing solid ceramic components with uniform layered radiation drying *Addit. Manuf.* **15** 102–12
[135] Ebendorff-Heidepriem H, Schuppich J, Dowler A, Lima-Marques L and Monro T M 2014 3D-printed extrusion dies: a versatile approach to optical material processing *Opt. Mater. Express* **4** 1494
[136] Heng D O Z, An Y L I, Hen E R H U C, Eibei B L I, Ong D E K, Ei W L I and Ian J W U 2016 Free-space to few-mode-fiber coupling under atmospheric turbulence *Opt. Express* **24** 18739–44
[137] Huang Y, Xu Y and Yariv A 2004 Fabrication of functional microstructured optical fibers through a selective-filling technique *Appl. Phys. Lett.* **85** 5182–4
[138] De M and Singh V K 2018 Magnetic fluid infiltrated dual core photonic crystal fiber based highly sensitive magnetic field sensor *Opt. Laser Technol.* **106** 61–8
[139] Xiao L, Jin W, Demokan M, Ho H, Hoo Y and Zhao C 2005 Fabrication of selective injection microstructured optical fibers with a conventional fusion splicer *Opt. Express* **13** 9014–22
[140] Wang Y, Liao C R and Wang D N 2010 Femtosecond laser-assisted selective infiltration of microstructured optical fibers *Opt. Express* **18** 18035
[141] Wang F, Yuan W, Hansen O and Bang O 2011 Selective filling of photonic crystal fibers using focused ion beam milled microchannels *Opt. Express* **19** 17585
[142] Andrade G F S and Brolo A G 2012 Nanoplasmonic structures in optical fibers *Nanoplasmonic Sensors* (Berlin: Springer) pp 289–315
[143] Atakaramians S, Afshar V S, Ebendorff-Heidepriem H, Nagel M, Fischer B M, Abbott D and Monro T M 2009 THz porous fibers: design, fabrication and experimental characterization *Opt. Express* **17** 14053
[144] Yuan W, Khan L, Webb D J, Kalli K, Rasmussen H K, Stefani A and Bang O 2011 Humidity insensitive TOPAS polymer fiber Bragg grating sensor *Opt. Express* **19** 19731
[145] De M, Gangopadhyay T K and Singh V K 2019 Prospects of photonic crystal fiber as physical sensor: an overview *Sensors* **19** 464
[146] Mahdiraji G A, Amirkhan F, Chow D M, Kakaie Z, Yong P S, Dambul K D and Adikan F R M 2014 Multicore flat fiber: a new fabrication technique *IEEE Photonics Technol. Lett.* **26** 1972–4
[147] Egorova O, Astapovich M, Semenov S and Salganskii M 2014 Multicore optical fiber with rectangular cross-section *Opt. Lett.* **39** 2168–70
[148] Armelao L, Barreca D, Bottaro G, Bruno G, Gasparotto A, Losurdo M and Tondello E 2005 RF-sputtering of gold on silica surfaces: evolution from clusters to continuous films *Mater. Sci. Eng.* C **25** 599–603
[149] Ziblat R, Lirtsman V, Davidov D and Aroeti B 2006 Infrared surface plasmon resonance: a novel tool for real time sensing of variations in living cells *Biophys. J.* **90** 2592–9
[150] Dash J N and Jha R 2015 On the performance of graphene-based D-shaped photonic crystal fibre biosensor using surface plasmon resonance *Plasmonics* **10** 1123–31